



Morphology and paleobiology of the Late Cretaceous large-sized shark *Cretodus crassidens* (Dixon, 1850) (Neoselachii; Lamniformes)

Authors: Amalfitano, Jacopo, Dalla Vecchia, Fabio Marco, Carnevale, Giorgio, Fornaciari, Eliana, Roghi, Guido, et al.

Source: Journal of Paleontology, 96(5) : 1166-1188

Published By: The Paleontological Society

URL: <https://doi.org/10.1017/jpa.2022.23>


BioOne Complete (complete.BioOne.org) is a full-text database of 200 subscribed and open-access titles in the biological, ecological, and environmental sciences published by nonprofit societies, associations, museums, institutions, and presses.

Your use of this PDF, the BioOne Complete website, and all posted and associated content indicates your acceptance of BioOne's Terms of Use, available at www.bioone.org/terms-of-use.

Usage of BioOne Complete content is strictly limited to personal, educational, and non - commercial use. Commercial inquiries or rights and permissions requests should be directed to the individual publisher as copyright holder.

BioOne sees sustainable scholarly publishing as an inherently collaborative enterprise connecting authors, nonprofit publishers, academic institutions, research libraries, and research funders in the common goal of maximizing access to critical research.

Morphology and paleobiology of the Late Cretaceous large-sized shark *Cretodus crassidens* (Dixon, 1850) (Neoselachii; Lamniformes)

Jacopo Amalfitano,^{1*}  Fabio Marco Dalla Vecchia,² Giorgio Carnevale,³ Eliana Fornaciari,¹ Guido Roghi,⁴ and Luca Giusberti¹

¹Dipartimento di Geoscienze, Università degli Studi di Padova, Padova I-35131, Veneto, Italy <jacopo.amalfitano@unipd.it> <eliana.fornaciari@unipd.it> <luca.giuberti@unipd.it>

²Institut Català de Paleontologia (ICP), Universitat Autònoma de Barcelona, Cerdanyola del Vallès E-08193, Catalunya, Spain <fabio.dallavecchia@icp.cat>

³Dipartimento di Scienze della Terra, Università degli Studi di Torino, Torino I-10125, Piemonte, Italy <giorgio.carnevale@unito.it>

⁴Istituto di Geoscienze e Georisorse, CNR, Padova I-35131, Veneto, Italy <guido.roghi@igg.cnr.it>

Abstract.—The definition of the Cretaceous shark genus *Cretodus* Sokolov, 1965 is primarily based on isolated teeth. This genus includes five species. Among these, *Cretodus houghtonorum* Shimada and Everhart, 2019 is the only species based on a partially preserved skeleton. Here, the taxonomic attribution of a virtually complete skeleton of *Cretodus* from the Turonian of northeastern Italy is discussed, together with a few specimens from the Turonian of England. One of the latter is investigated through micropaleontological analysis to determine its stratigraphic position. The material is referred to *Cretodus crassidens* (Dixon, 1850), the diagnosis of which is emended herein. The dentition is tentatively reconstructed, exhibiting strong similarities with congeneric species, although it differs in having strong vertical folds on the main cusp labial face, a mesiodistally broad tooth aspect, weak and well-spaced ‘costulae’ at crown base, and a different dental formula in the number of parasymphyseal and lateral rows. Some tooth malformations are interpreted as feeding-related or senile characters. The Italian specimen suggests that *Cretodus crassidens* had a wide and laterally expanded mouth and head, a stout body, and attained a gigantic size. *Cretodus crassidens* was a moderate-speed swimming shark ecologically like the extant tiger shark *Galeocerdo cuvier* (Péron and Lesueur in Lesueur, 1822). The age estimate from vertebral-band counting suggests that the Italian individual was at least 23 years old and the growth model indicates a longevity of 64 years and a maximum attainable total length of 9–11 m. *Cretodus crassidens* occurs both in Boreal and Tethyan domains, implying a broad paleobiogeographic distribution and a preference toward offshore settings.

Introduction

The extinct shark *Cretodus* Sokolov, 1965, like many other extinct chondrichthyans, was defined based on isolated teeth collected from Upper Cretaceous (Cenomanian–Turonian) marine deposits from all over the world (Cappetta, 2012). However, this large lamniform is also represented by associated skeletal remains recently reported from the middle-upper Turonian Scaglia Rossa of Veneto, northeastern Italy (Amalfitano et al., 2017a) and from the middle Turonian Blue Hill Shale Member of the Carlisle Shale of Kansas, USA (Shimada and Everhart, 2019). The partial skeleton from Kansas was assigned to a new species, *Cretodus houghtonorum* Shimada and Everhart, 2019, whereas the Italian specimen has been regarded since its discovery as close to *Cretodus crassidens* (Dixon, 1850). Amalfitano et al. (2017a) prudently referred the Italian specimen to *Cretodus* sp. in a study focused on a pellet-like accumulation

of turtle bones alongside the vertebral column of the shark, which was interpreted as its gastric content. Based on dental characters, Shimada and Everhart (2019) considered the specimen discussed by Amalfitano et al. (2017a) to be conspecific with, or closely allied to, *Cretodus crassidens*. The attribution to *Cretodus crassidens* is confirmed herein based on a detailed analysis of the Italian specimen and further supported by additional information and comparison with other material, including the holotype, from the English Chalk Group of southern England, UK. A tentative reconstruction of the dentition of this species is also provided here, together with a discussion on several paleobiological traits of the species.

Geological setting

The geological setting of the ‘Lastame’ lithofacies of the Scaglia Rossa of the Lessini Mountains (~30 km N of Verona, Veneto, Italy; Fig. 1), which yielded the *Cretodus* remains, has been thoroughly described in a series of papers dealing with the remarkable vertebrate assemblage of this Cretaceous Lagerstätte

*Corresponding author.

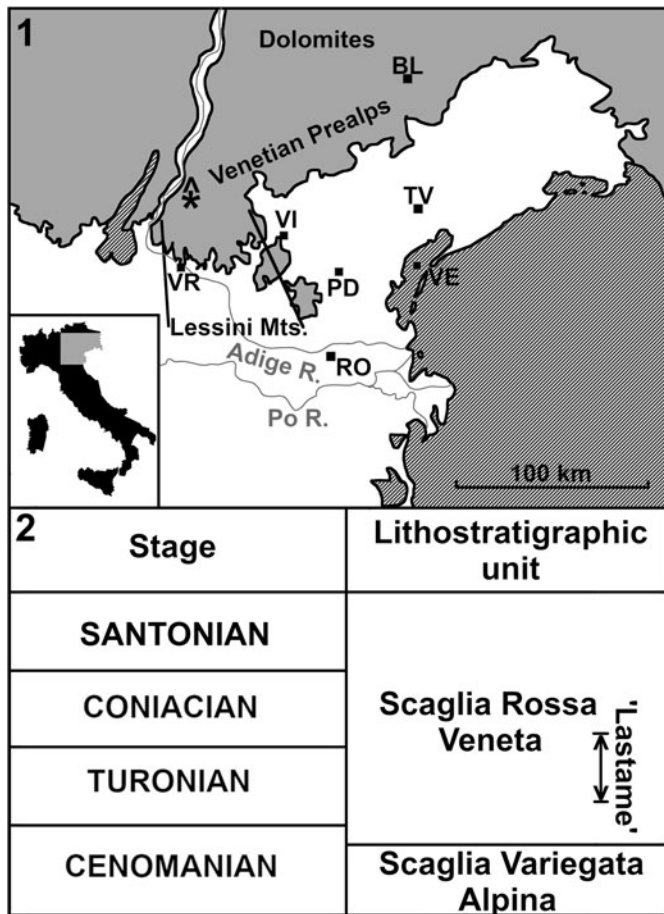


Figure 1. (1) Simplified location map and lithostratigraphic context of the 'Lastame' localities. The quarries are located on Mt. Loffa (Lessini Mountains, Verona Province). (2) Lithostratigraphic chart summarizing Cenomanian–Santonian formations of northeastern Italy. 'Lastame' spans from Turonian pro parte to Coniacian pro parte. BL = Belluno; PD = Padova; RO = Rovigo; TV = Treviso; VE = Venezia; VI = Vicenza; VR = Verona; * = location of the Benedetti quarry yielding the Italian specimen of *Cretodus crassidens*; gray = mountain ranges or hills; white = plains and valleys.

(Amalfitano et al., 2017a, b, 2019; Amadori et al., 2019, 2020a, b; Palci et al., 2013). The 7 m thick nodular/subnodular interval of whitish and pinkish-reddish limestones of the Scaglia Rossa extensively quarried in Verona Province is characterized by abundant echinoids, inoceramids, ammonoids, and rudists, but also by vertebrate remains, e.g., lamniform sharks, sclerorhynchiforms, bony fishes, marine turtles, and mosasaurs. The Lastame spans from Turonian p.p. to Coniacian p.p. (e.g., Cigala-Fulgosi et al., 1980; Trevisani and Cestari, 2007; Walliser and Schöne, 2020), but most of the vertebrate skeletons and partial remains so far investigated comes from the middle-upper Turonian interval (e.g., Amalfitano et al., 2017a, b, 2019; Amadori et al., 2020a, b).

The *Cretodus* remains from southern England (UK) examined herein come from the Upper Cretaceous Chalk of Kent (especially near the town of Lewes; Fig. 2.1) and surrounding counties. The associated remains are referred to the classic 'Middle Chalk Group' of southern England (Hopson, 2005). This unit is part of the Chalk Group, specifically the White Chalk Subgroup, deposited in the northwestern part of the Anglo-Paris

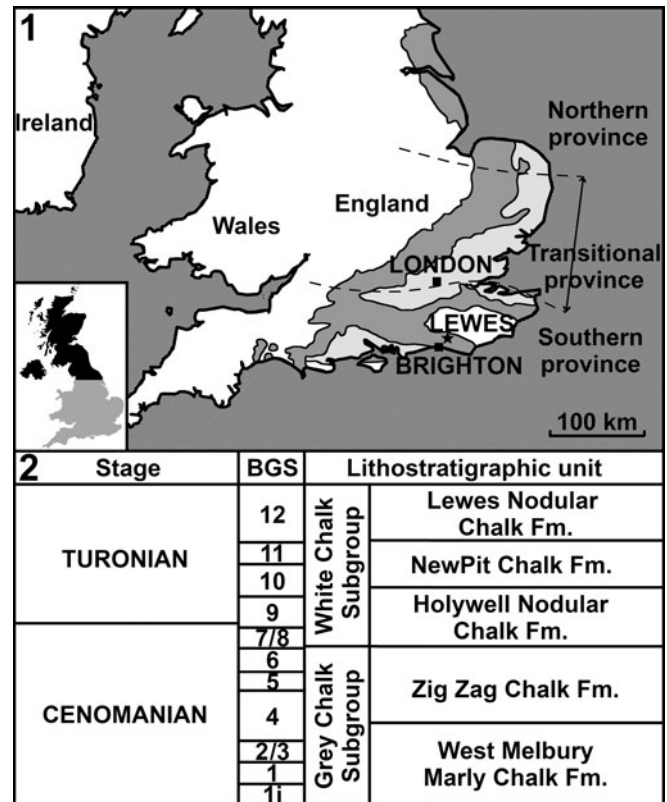


Figure 2. (1) Simplified location map of the English Chalk. Cretaceous rocks at outcrop (dark gray) and concealed (light gray) in England. (2) Lithostratigraphic chart summarizing the Cenomanian–Turonian formations of the Chalk Group. BGS = British Geological Survey, Fm. = Formation. Modified after Hopson (2005) and Wilkinson (2011).

Basin and equivalent to the lowest part of the Lewes Nodular Chalk Formation, the New Pit Chalk Formation, and the Holywell Nodular Chalk Formation (with the exclusion of the Plenus Marls Member) in the Southern Province (Hopson, 2005; Wilkinson, 2011; Gale, 2019; Fig. 2.2). The 'Middle Chalk' spans from the upper Cenomanian (only the Plenus Marl Member) to the middle Turonian (Wilkinson, 2011) and yielded remains of numerous fossil fish taxa, although the number of vertebrates per volume of rock is very low (Mantell, 1822; Woodward, 1902, 1903, 1907, 1908, 1909, 1911, 1912; Kriwet, 2002; Friedman et al., 2016); the ichthyofauna therein includes a large variety of bony fishes (e.g., Dixon, 1850; Woodward, 1902, 1903, 1907, 1908, 1909, 1911, 1912; Kriwet, 2002) and several cartilaginous fishes (e.g., *Cretoxyrhina* and *Ptychodus*; Dixon, 1850; Woodward, 1902, 1903, 1907, 1908, 1909, 1911, 1912; Longbottom and Patterson, 2002).

Materials and methods

The material studied herein consists of a partial articulated skeleton (101 teeth, two segments of 86 disconnected and coin-stacked vertebral centra and fragments of cranial mineralized cartilage) from the Scaglia Rossa exhibited at the Paleontological and Prehistorical Museum 'Don Alberto Benedetti' (Museo Paleontologico e Preistorico) of Sant'Anna d'Alfaedo, Verona Province, Italy (MPPSA IGVR 91032) and some

specimens from the Chalk Group of southern England (UK). The English material includes a disturbed tooth set with a single vertebral centrum housed at the Booth Museum of Natural History of Brighton, England, UK (BMB 007312), and a disarticulated tooth set (NHMUK PV OR 25786) and several isolated teeth that belong to the collections of The Natural History Museum of London (NHMUK PV OR 25823 [holotype of *Cretodus crassidens*], 41704, 49951, 44623, and NHMUK PV P 4577, 5402, 11144, 12368, 12860, 12870).

The specimens were photographed using a Nikon D810 camera with a 60–90 mm lens and a Canon PowerShot SX720 HS. Measurements were retrieved through the image analysis software ImageJ (<https://imagej.nih.gov/ij/>, v. 1.6; Schneider et al., 2012). Images and interpretative drawings of the specimens were produced using the free software packages GIMP (GNU Image Manipulation Program, <https://www.gimp.org/>, v. 2.10.6) and Inkscape (<https://inkscape.org/>, v. 0.92). The synonymy list follows the standards proposed by Matthews (1973) and include selected synonyms directly referring to the material described herein. The growth model was reconstructed using the software package Past 3.26 (<https://past.en.lo4d.com/windows>; Hammer et al., 2001) and plotted with the Desmos graphing software (<https://www.desmos.com/>).

The reconstruction of the dentition of *Cretodus crassidens* provided herein is based on the disarticulated dentition of the Italian specimen MPPSA IGVR 91032, therefore might be subject to biases such as taphonomic or preparation loss and interpretation bias. Specimen MPPSA IGVR 91032, in fact, was discovered between 1996 and 1997 by quarry owners Giovanni and Gianfranco Benedetti and was prepared by Giovanni Benedetti in 2003 (Amalfitano et al., 2017a). According to the preparator, the two slabs come from the same layer and were separated by a karst fissure; thus, the skeletal remains in the two slabs should belong to the same individual. Nevertheless, the two slabs differ slightly in color and the different sizes between the last vertebral centrum on the main slab and the first centrum on the second slab suggest that several vertebrae are missing between the two segments (Amalfitano et al., 2017a). Furthermore, the vertebrae on the second slab are all glued. Most of the teeth (~70%) detached from slab A when it was exposed by quarry works or remained attached to the counterslab (now missing); they were glued onto the slab later and mostly not in their exact original position (some might be lost). However, the glued teeth undoubtedly belong to this specimen because their morphological characters are identical to the in-situ teeth (Amalfitano et al., 2017a). The teeth are figured only on the labial side or the lingual side because most of them are still embedded in the sedimentary matrix or were glued after detaching and are exposed mainly on one side. Chemical or physical preparation to separate the teeth from the matrix (e.g., Siversson et al., 2007), as well as sectioning the vertebral centra (e.g., Newbrey et al., 2015; Shimada and Everhart, 2019), was not possible because the specimen is subject to Italian cultural heritage care laws and cannot be altered without special permission. Ammonium chlorite coating of the teeth (e.g., Siversson et al., 2007; Amadori et al., 2019) was also not performed because of technical issues related to the position and size of the specimen in the Museum exhibition. Teeth in the reconstruction are illustrated from the left side of the jaws and missing elements were filled with mirrored images of teeth from the

right side. Tooth numbering of MPPSA IGVR 91032 in the text, figures, and tables is consistent with that of Amalfitano et al. (2017a, fig. 6). Some correction of the tooth measurements of MPPSA IGVR 91032 and new tooth measurements of BMB 007312 are provided in Appendices 1 and 2.

Except for the uninformative calcified cartilage fragments, the morphology of each anatomical element is described and figured in detail herein. Terminology and abbreviations follow usual standards for shark teeth, placoid scales, and vertebral centra (e.g., Ridewood, 1921; Shimada, 1997a, b, c; Siversson, 1999; Cappetta, 2012; Newbrey et al., 2015; Shimada and Everhart, 2019). Nevertheless, the symphyseal teeth sensu Shimada and Everhart (2019) are referred herein as parasymphyseal teeth, and the intermediate teeth from the same paper as third anterior teeth following Siversson's (1999) terminology. In the literature of fossil lamniforms, teeth near the symphysis have been consistently addressed as symphyseal teeth (e.g., Siversson, 1999; Shimada, 2002). However, Lamniformes all lack symphyseal teeth (Smith et al., 2013), therefore the erroneous use in dental nomenclature of symphyseal teeth in Lamniformes should be replaced by the term parasymphyseal teeth, already used in other papers (e.g., Cook et al., 2011; Siversson et al., 2013). The intermediate position sensu Applegate (1967) refers to teeth arising from the area (intermediate bar) between the hollows (bullae) where the other teeth accommodate in the odontaspidid dentition, but the majority of lamniforms do not exhibit this condition, having two separate hollows in the upper jaw without teeth on the intermediate bar and a single hollow in the lower jaw (e.g., Siversson, 1999).

A least square linear regression method was applied to the vertebral centrum length data to estimate the original vertebral count of the shark and to provide a length estimate of MPPSA IGVR 91032 (modelled in Past 3.26, Supplemental Data 1; data from Amalfitano et al., 2017a, appendix B). Tooth size is usually employed as a parameter to infer total length of a fossil or extant shark, considering both crown or tooth height (e.g., Gottfried et al., 1996; Shimada, 2003, 2019) and tooth width. Tooth width exhibits less variability than crown height (Bass et al., 1975) and thus has been considered more reliable by several authors (e.g., Newbrey et al., 2015; Perez et al., 2021). In this paper, we considered both methods, despite that the total jaw width method is not directly applicable because of poor preservation of most of the tooth roots in the sample considered herein. Length estimates are provided using the equation by Shimada and Everhart (2019) that exploits the theoretical linear relationship of crown height (CH) and total length (TL) for *Cretoxyrhina mantelli* (see Shimada, 2008, fig. 5):

$$TL(\text{cm}) = 12.5 \times CH(\text{mm}) \quad (1)$$

However, Shimada et al. (2020) provided a more conservative estimate based on the linear function:

$$TL(\text{cm}) = 11.784 \times CH(\text{mm}) - 0.331 \quad (2)$$

with CH of any anterior tooth in any given non-*Alopias* macrophagous lamniform taxon, although this possibly underestimated the body total length.

Using the definition of bite circumference sensu Lowry et al. (2009) to bypass the lack of a reliable total jaw width and applying the reverse of their formula:

$$\begin{aligned} \log(\text{bite 'circumference'}[\text{mm}]) \\ = 1.007 \times \log(\text{TL}[\text{mm}]) - 0.8 \end{aligned} \quad (3)$$

for the great white shark *Carcharodon carcharias* (Linnaeus, 1758), it is possible to have a TL estimate of *Cretodus crassidens* also from the arch-like arrangement of teeth in specimen MPPSA IGVR 91032 (geometrical approximation in Supplemental Data 2).

An attempt to assess the growth pattern of the fossil shark using the von Bertalanffy growth function (VBGF; von Bertalanffy, 1938) is proposed below. The VBGF has been widely used to describe the growth of fish (Haddon, 2001). This function was specifically used as a quantitative method to describe the growth of extant elasmobranchs based on growth bands on calcified structures such as vertebral centra (e.g., Cailliet and Goldman, 2004; Goldman, 2004). The method has also been applied to some extinct sharks (e.g., Shimada, 2008; Cook et al., 2011; Newbrey et al., 2015; Shimada and Everhart, 2019; Jambura and Kriwet, 2020; Shimada et al., 2021). The VBGF provides the best fit for species with slow growth and extended longevity (maximum total length >100 cm of total length and $0.02 < k < 0.25 \text{ yr}^{-1}$, where k is the growth coefficient), such as large pelagic sharks (Liu et al., 2021). It must be mentioned that conventional VBGF analyses uses independent measurements from a dataset with many random samples from a population. The VBGF method applied here exploits original and derived measurements (Table 1) from a single but best-preserved specimen, that would be considered dependent measurements. This exploratory method has been recently applied in other papers (e.g., Shimada and Everhart, 2019; Shimada

et al., 2021) and has proven to be a viable approach to attempt to explore the growth pattern of extinct elasmobranchs, although with the obvious limits dependent from the restricted sample. Parameters obtained from the VBGF and other derived measurements are applied with equations from Natanson et al. (2006) for longevity to discuss and compare the results of the analyses.

Specimen BMB 007312 is still embedded in Chalk soft matrix. The matrix was hence collected as powdered residual fallen from the specimen after simple handling. The sample was prepared as unprocessed material on a smear slide and examined under a light microscope at 1250X magnification to establish the stratigraphic position of the specimen. The calcareous nannofossil content of the samples was analyzed with semiquantitative methods (three vertical traverses corresponding to 6–7 mm²) following Gardin and Monechi (1998).

Repositories and institutional abbreviations.—Types, figured, and other specimens examined in this study are deposited in the following institutions: Booth Museum of Natural History of Brighton, UK (BMB); Sternberg Museum of Natural History, Fort Hays State University, Hays, Kansas, USA (FHSM); Museo Paleontologico e Preistorico di Sant'Anna d'Alfaedo, Verona, Italy (MPPSA IGVR); and The Natural History Museum, London, UK (NHMUK).

Systematic paleontology

Class Chondrichthyes Huxley, 1880
 Subclass Elasmobranchii Bonaparte, 1838
 Cohort Euselachii Hay, 1902
 Subcohort Neoselachii Compagno, 1977
 Order Lamniformes Berg, 1958
 Family Pseudoscapanorhynchidae Herman, 1979 (sensu Siversson and Machalski, 2017)
 Genus *Cretodus* Sokolov, 1965 (sensu Shimada and Everhart, 2019)

Type species.—*Otodus sulcatus* Geinitz, 1843; 'unterer Plänen (plenus-marl), upper part of upper Cenomanian, Plauen, Saxony, Germany.

Cretodus crassidens (Dixon, 1850)
 Figures 3–10

Selected synonymy:

†1850 *Oxyrhina crassidens* Dixon, p. 367, pl. 31, figs. 13, 13A.
 1889 *Oxyrhina crassidens*; Woodward, p. 382.
 1911 *Oxyrhina crassidens*; Woodward, p. 205, pl. 44, figs. 1, 2.
 1987 *Cretodus crassidens*; Cappetta, p. 98.
 2012 *Cretodus crassidens*, Cappetta, p. 255.
 2017a *Cretodus* sp.; Amalfitano et al., p. 109, figs. 2, 4, 6–9, 15.
 2019 *Cretodus crassidens*; Shimada and Everhart, p. 4, fig. 9A–P.

Holotype.—NHMUK PV OR 25823 (isolated tooth).

Diagnosis (emended).—A *Cretodus* species that differs from all other species of the genus by teeth with mesiodistally broad

Table 1. Raw measurements (BN, CR) and derived measurements (pCR, TL₁, TL₂, and CH) based on a vertebral centrum of *Cretodus crassidens* (Dixon, 1850) (MPPSA IGVR 91032; Fig. 11). BN = band pair number; CH = crown height; CR = center radius; pCR = percentage of center radius; TL = total length.

BN	CR (mm)	pCR (%)	TL ₁ (cm)	TL ₂ (cm)	CH (mm)
0	10.7	21.5	141.9	167.7	12.0
1	14.1	28.5	187.8	221.9	15.9
2	16.9	34.0	224.3	265.1	19.0
3	19.4	39.1	258.1	305.0	21.9
4	21.4	43.2	285.1	336.9	24.2
5	23.5	47.3	312.1	368.9	26.5
6	25.5	51.4	339.1	400.8	28.8
7	27.3	55.0	362.8	428.7	30.8
8	29.1	58.6	387.1	457.5	32.8
9	30.8	62.1	410.0	484.6	34.8
10	32.7	65.8	434.4	513.4	36.9
11	34.5	69.5	458.7	542.1	38.9
12	36.5	73.6	485.7	574.0	41.2
13	38.0	76.5	504.6	596.4	42.8
14	39.2	78.9	520.8	615.5	44.2
15	40.7	82.0	541.1	639.5	45.9
16	42.4	85.5	564.1	666.6	47.9
17	44.4	89.4	589.8	697.0	50.0
18	45.3	91.2	601.9	711.3	51.1
19	46.3	93.2	615.4	727.3	52.2
20	47.2	95.1	627.6	741.7	53.2
21	48.0	96.7	638.4	754.5	54.2
22	48.7	98.2	647.8	765.6	55.0
23	49.6	100.0	660.0	780.0	56.0

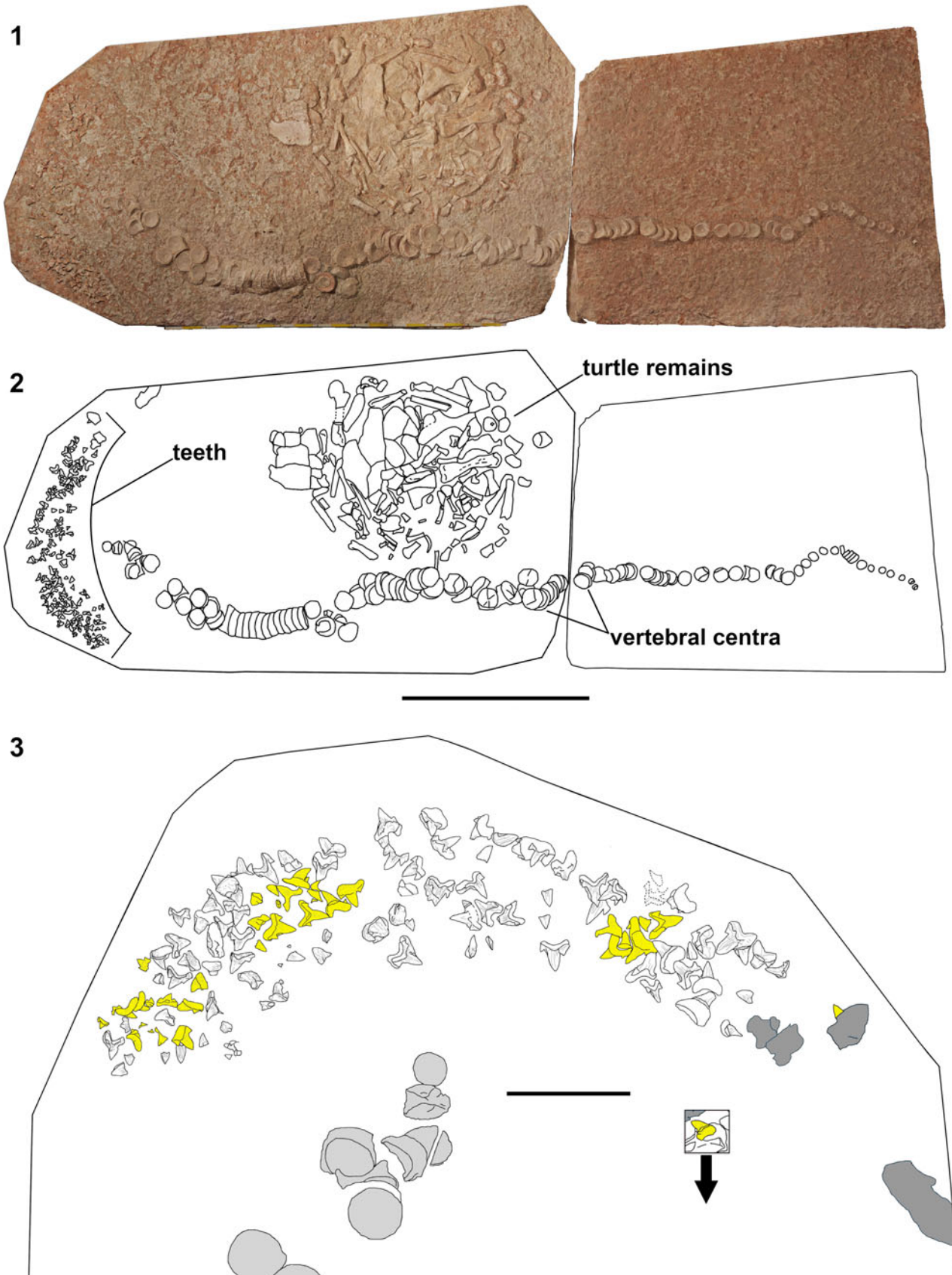


Figure 3. Partial articulated skeleton of *Cretodus crassidens* (Dixon, 1850) from the middle Turonian of the Scaglia Rossa Veneta of northeastern Italy, MPPSA IGVR 91032: (1) Orthophoto of the specimen. The slab embedding the tooth accumulation, the tessellated cartilage elements, the anterior portion of the vertebral column, and the turtle remains is Slab A. The one embedding the caudalmost vertebral centra is Slab B. (2) Interpretative drawing of (1). (3) Interpretative drawing of the tooth accumulation. Teeth in situ are indicated (yellow in electronic version), with tessellated cartilage elements (dark gray) and anteriormost vertebral centra (light gray). Scale bars = 1 m (1, 2), 20 cm (3).

aspect (crown width to 82% of crown height even in a2), slightly ogival to triangular main cusp, with vertical strong folds and deep grooves on the labial face, weak and well-spaced basal crown ‘costulae’ (or ‘striae’) on labial and lingual faces, robust lateral cusplets (lateral cusplet height ~25–55% of crown height), sinusoid to parabolic crown base and sinusoid to parabolic basal concavity. Aberrant lateral cusplets can be present or replaced by weakly crenulated heels on the shoulders of the main cusp or rounded papillae.

Occurrence.—The type locality is Houghton, Sussex (England, UK); the stratigraphic horizon is the ‘Middle Chalk,’ Turonian. All other English specimens come from localities of the ‘Middle Chalk’: Lewes, Sussex, and Whyteleafe, in Surrey (England, UK), although the exact geospatial coordinates are not known. The Italian specimen comes from the ‘Lastame’ lithofacies of Scaglia Rossa Veneta (middle-upper Turonian) of Mt. Loffa, Sant’Anna d’Alfaedo (Lessini Mountains, Veneto, Italy), specifically from Benedetti Quarry (45.6°N, 10.9°E).

The matrix obtained from BMB 007312 contains abundant and well-preserved calcareous nannofossils. The assemblage is well-diversified and contains 13 specimens of *Lucianorhabdus maleformis* Reinhardt, 1966, four specimens of *Quadrum gartneri* Prins and Perch-Nielsen in Manivit et al., 1977 in ~6 mm², that, together with the absence of *Eiffellithus eximius* s.s. Huber et al., 2017 (only one uncertain specimen) and *Lucianorhabdus quadrifidus* Forchheimer, 1972, are indicative of the Biozone UC 7 of Burnett (1999). The corresponding interval would be lower-middle Turonian. Correlation with the foraminiferal zonation of the Chalk Group allows assignment of the sample to the *Helvetoglobotruncana helvetica* Biozone and possibly the lower part of the *Marginotruncana sigali* Biozone, corresponding to the British Geological Survey (BGS) Zones 9–10 (Wilkinson, 2011; Huber et al., 2017). Based on biostratigraphic data, the sample is placed between the middle-upper part of the Holywell Nodular Chalk Formation and basal part of the New Pit Chalk Formation.

Description.—The English specimens include mainly isolated teeth, previously reported by Woodward (1911) under various names. There are also several associated specimens: the disarticulated tooth set NHMUK PV 25786 (including seven disarticulated teeth), the disturbed tooth set BMB 007312 and the Italian specimen MPPSA IGVR 91032 (Figs. 3, 4, 8–11). The English specimen BMB 007312 includes 18 teeth, nine still embedded in matrix, associated with two vertebral centra, one fragmentary and the other complete and undeformed, characterized by maximum diameter 95 mm and thickness ~40 mm; this specimen was possibly reported as ‘a small group of associated teeth from Lewes’ by Woodward (1911, p. 206; Figs. 5, 6). The Italian specimen MPPSA IGVR 91032 is a virtually complete articulated skeleton that includes 120 teeth, 86 vertebral centra, as well as fragments of cranial mineralized cartilage. This specimen also preserves placoid scales retrieved from residues processed from matrix samples, and includes a circular accumulation of bones of a marine turtle alongside the shark vertebral column, interpreted as a gastric pellet (Amalfitano et al., 2017a). Dental characters and other morphological features are described in detail below.

Materials.—NHMUK PV OR 25786 (disarticulated tooth set, sensu Shimada, 2005), 41704, 49951, 44623; NHMUK PV P 4577, 5402, 11144, 12368, 12860, 12870; BMB 007312 (disturbed tooth set, sensu Shimada, 2005); MPPSA IGVR 91032.

Remarks.—The dental characters of the specimens described above are fully consistent with the diagnosis of *Cretodus* proposed by Shimada and Everhart (2019). In this paper, an emended diagnosis is introduced specifying new details observed on the materials analyzed.

The anatomy of *Cretodus crassidens*

Teeth.—Some of the most representative teeth are illustrated in Figure 4; a reconstruction of the dentition is illustrated in Figure 7. Here follows a description of general dental characters and an interpretation of the tooth pattern within the upper and lower series, considering that the specimen IGVR 91032 preserves a largely disarticulated dentition.

General characters.—Teeth mesiodistally broad (crown width to 82% of crown height even in anterior teeth, specifically a2), with main cusp and a pair of large lateral cusplets, the mesial one divergent and the distal one slightly convergent with respect to main cusp (can be divergent in some teeth). Main cusp is massive, slightly ogival to triangular, with strong vertical folds and two to five deep grooves on labial face. Lateral teeth have triangular main cusp. Lateral cusplets are well separated from main cusp but connected on labial side with basally extended crown base on both root lobes. Numerous, regularly and well-spaced, well-marked, and very short vertical grooves and ridges (‘costulae’ or ‘striae’) are present at crown base on both labial and lingual sides, more marked on labial side. Cutting edges are usually continuous and sharp, connecting main cusp and cusplets. Mesial root lobe is usually slightly pointed, whereas distal lobe is more expanded and rounded. Labial face of root is flat or slightly recessed at crown base. Lingual face of root is overall swollen and bulgy, with lingual protuberance (more evident and protruding in parasymphyseals, anteriors, and mesialmost laterals). Lateral teeth exhibit more splayed root lobes than parasymphyseals and anteriors.

Upper dentition.—Upper teeth are labiolingually thick, massive, and almost straight, with convex labial and lingual faces and tip slightly turned outward in certain specimens. Cutting edges are straight and continuous. Crown base and basal root concavity are deeply sinusoid (especially in anterior teeth). Root-lobes angle is acute in parasymphyseals and anteriors, and is right in laterals. Root lobe apices are directed basally. The upper dentition includes two parasymphyseal rows, three anterior rows, and at least 10 lateral rows, but a large gap is present after L8 (possibly two missing rows). Distinctive characters of tooth rows are:

- (1) Upper parasymphyseal teeth (P): Main cusp is rather slender (PCH-PCW ratio 1.4–1.5). P1 exhibits a mesially curved main cusp. P2 almost straight and is the smallest among these teeth. The height of the lateral cusplet represents 32% of crown height.

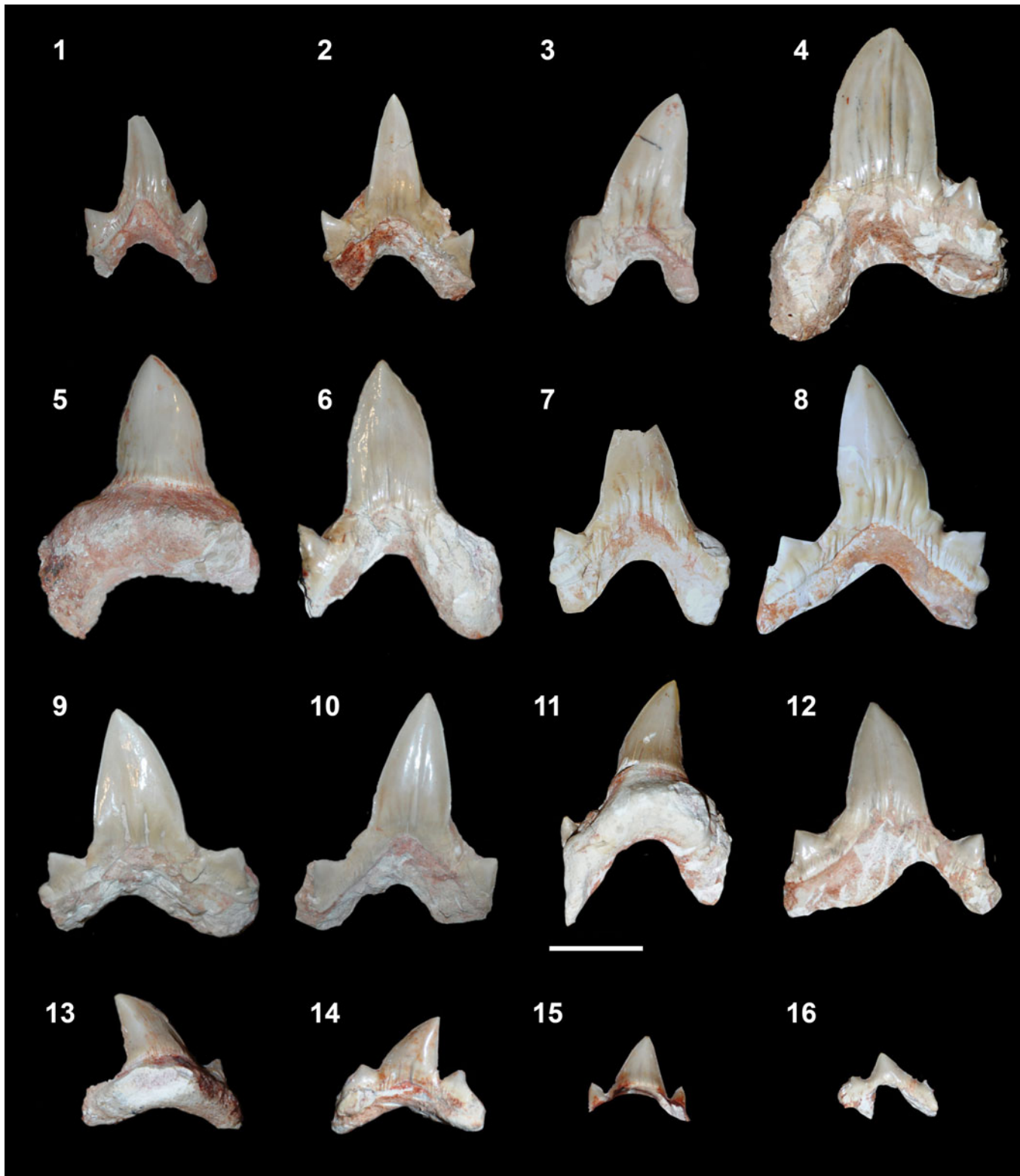


Figure 4. Selection of representative teeth of *Cretodus crassidens* (Dixon, 1850) from the middle Turonian of the Scaglia Rossa Veneta of northeastern Italy, MPPSA IGVR 91032: (1) first upper parasymphyseal tooth (no. 16), labial view; (2) first lower parasymphyseal tooth (no. 22), labial view; (3) first upper anterior tooth (no. 37), labial view; (4) second lower anterior tooth (no. 3), labial view; (5) second lower anterior tooth (no. 11), lingual view; (6) second upper anterior tooth (no. 13), labial view; (7) third upper anterior tooth (no. 53), labial view; (8) third lower anterior tooth (no. 24), labial view; (9) first lower lateral tooth (no. 62), labial view; (10) third lower lateral tooth (no. 59), labial view; (11) sixth upper lateral tooth (no. 20), lingual view; (12) fourth upper lateral tooth (no. 61), labial view; (13) seventh lower lateral tooth (no. 103), lingual view; (14) eighth lower lateral tooth (no. 94), labial view; (15) ninth lower lateral tooth (no. 92), lingual view; (16) commissural upper lateral tooth (no. 104), labial view. Numbers match those used by Amalfitano et al. (2017a, fig. 6). Scale bar = 20 mm.

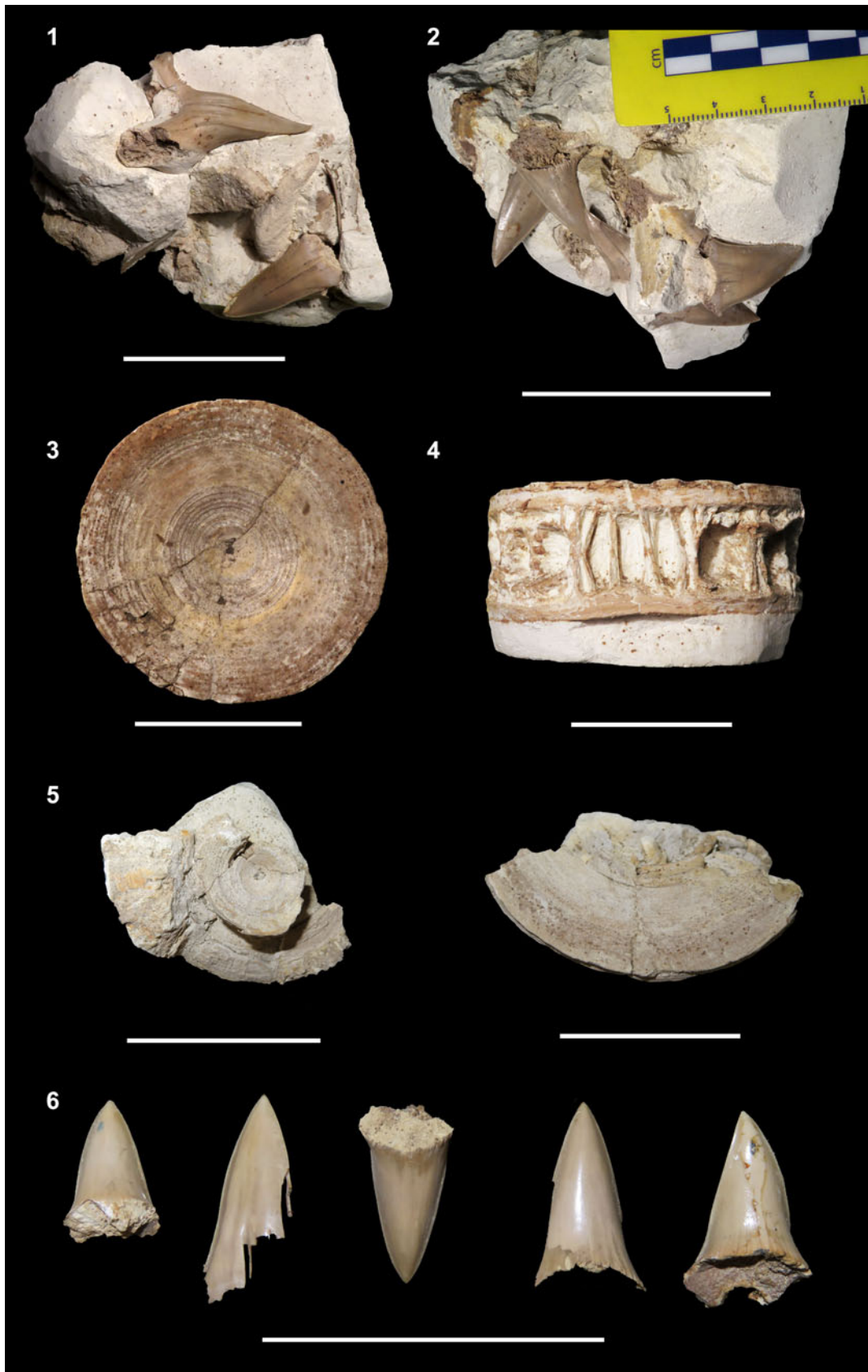


Figure 5. Associated remains of *Creodus crassidens* (Dixon, 1850) from the lower Turonian of the Chalk Group of England, BMB 007312: (1, 2) blocks with embedded teeth; (3, 4) complete vertebral centrum in frontal and dorsal views; (5) two fragments of a partial vertebral centrum in frontal view; (6) isolated teeth from the same tooth set (second one from left in labial view, all others in lingual view). Scale bars = 50 mm.

- (2) Upper anterior teeth (A): A1 is reduced (maximum observed height 51 mm) and strongly oblique distally (21° referring to the vertical axis). A2 and A3 have almost upright and apparently symmetrical main cusps; A2 is imperceptibly slanted mesially, and A3 distally. These teeth are rather large (A2 is 61 mm total height, the largest one of upper anteriors) and slender (TH-TW ratio 1.3–1.4). The root lobes of A1 are less splayed with respect to those of the adjacent teeth and U-shaped. The height of the lateral cusplet is $\sim 28\text{--}33\%$ of crown height.
- (3) Upper lateral teeth (L): Main cusp slightly to strongly distally oblique. Their maximum height ranges from 48 to 16 mm. L1–L3 teeth have an almost upright main cusp, from L4 onward the inclination becomes more evident. L11?–L12? possibly represent the commissural teeth. Teeth are generally larger than high except for the first three, with L2 representing the highest tooth (like in many other lamniforms; Shimada, 2002); lateral cusplet height is $35\text{--}54\%$ of crown height, with the ratio increasing toward the commissural rows. Root lobes become generally more divergent distally.

Lower dentition.—Lower teeth have a sigmoid profile (labiolingual direction), nearly flat labial face, and convex lingual face; the tip has a reversed curvature, so that although most of the crown is curved inward toward the mouth cavity, the tip is turned outward (as also observed in other sharks; Frazzetta, 1988), which confers a more labiolingually compressed and curved aspect with respect to the upper teeth. Main cusp of lower teeth is generally mesiodistally broader than those of upper teeth. Crown base and root concavity are shallow and more parabolic than those of upper teeth. Cutting edges are sigmoid in profile. Crown base slightly overhangs the upper portion of the root, creating a shallow recess and conferring a slightly

inflated aspect. Root-lobes angle is almost right in parasymphysals and anteriors, obtuse in laterals. Root-lobes apices slightly diverge. Lower dentition includes a single parasymphysal row, three anterior rows, and at least eight lateral rows, with a gap in the posteriormost positions, including commissural teeth. Distinctive characters of tooth rows are:

- (1) Lower parasymphysal teeth (p): These two teeth have a rather symmetric outline and slender main cusp (PCH-PCW ratio 1.3). Lateral cusplets are strongly divergent. The lateral cusplet height is $\sim 21\text{--}26\%$ of crown height.
- (2) Lower anterior teeth (a): These are the largest teeth in the dentition (a1 is 67 mm high, whereas a2 is 69 mm high, although incompletely mineralized; in this case it could be higher; 56 mm high in crown height). Tooth a1 is more symmetrical than a2, which is slightly slanted in distal direction. Main cusp of a2 bears four deep enameloid folds on the labial face extending for almost its entire height. Tooth a2 enlarged (crown width to 82% of crown height). Lateral cusplets height is $25\text{--}31\%$ of crown height (similar to upper anterior ratio). Tooth a3 is rather large (60 mm TH in functional row), with main cusp slightly bent distally and divergent cusplets. Tooth as high as wide (TH-TW ratio 1.18–1.02). Lateral cusplet height is $\sim 29\%$ of crown height.
- (3) Lower lateral teeth (l): Main cusp is almost upright to slightly oblique. The inclination of the cusp increases distally. Total height ranges 32–53 mm, but this range does not include the distalmost rows (which comprises teeth with crown height measuring 22 mm, 17, and 17 mm, 18). Teeth l1–l4 are almost as large as high, with almost upright cusps. Observing the size of l8 compared with those of the corresponding upper laterals, it is possible to suggest that there are at least four missing rows in the commissural part of the lower dentition. Lateral cusplet height represents



Figure 6. Second lower anterior tooth of *Cretodus crassidens* (Dixon, 1850), BMB 007312: (1) labial view; (2) mesial view; (3) distal view; (4) lingual view. Arrow indicates a dental malformation (crenulation on the cutting edge between the distal cusplet and the main cusp). Scale bar = 50 mm.

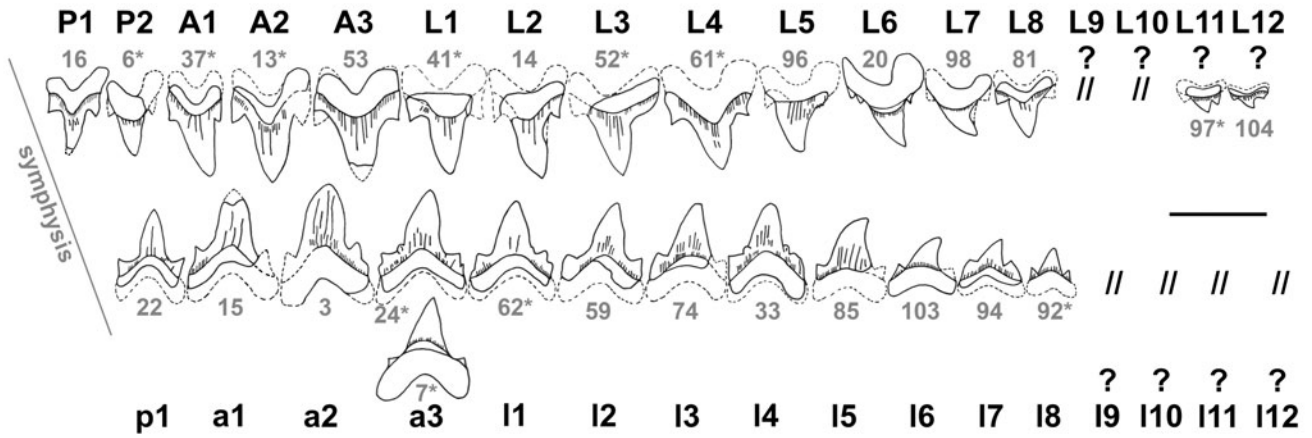


Figure 7. Interpretation of the dentition pattern in *Cretodus crassidens* (Dixon, 1850), based on specimen MPPSA IGVR 91032. Numbers in gray match those used by Amalfitano et al. (2017a, fig. 6). * = mirrored right teeth; dotted lines = reconstructed portions of the teeth based on other teeth in the sample; ? possibly missing tooth rows; // = gaps in the reconstruction. Scale bar = 50 mm.

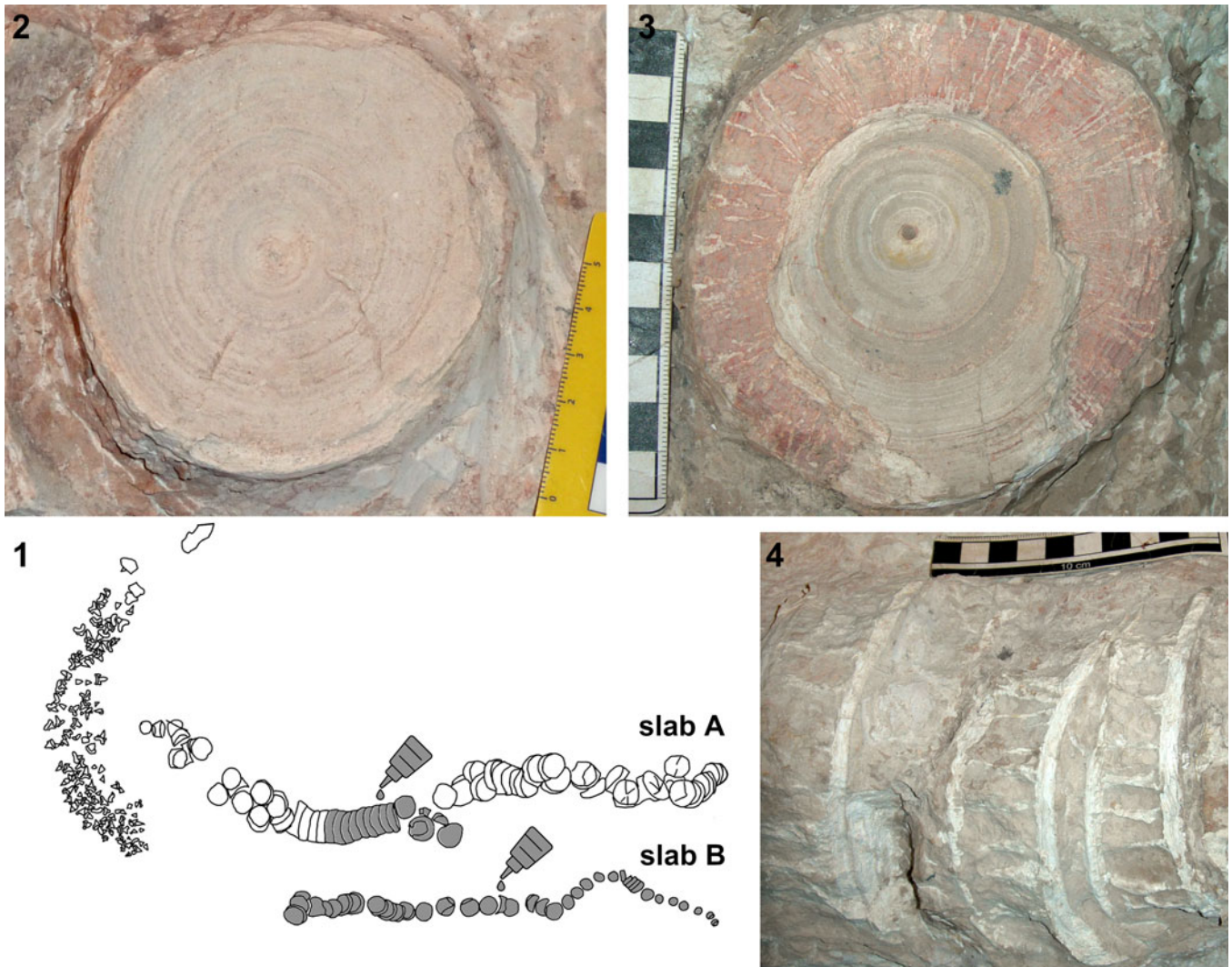


Figure 8. Vertebral centra of *Cretodus crassidens* (Dixon, 1850), MPPSA IGVR 91032: (1) interpretive drawing of slabs, with glued vertebral centra in dark gray; (2) exposed articular surface of corpus calcareum; (3) exposed intermedialia showing pattern of calcification of the vertebral centrum, showing radial and concentric lamellae patterns; (4) lateral side of vertebral centra exhibiting septae. Black and white scale bars in centimeters.

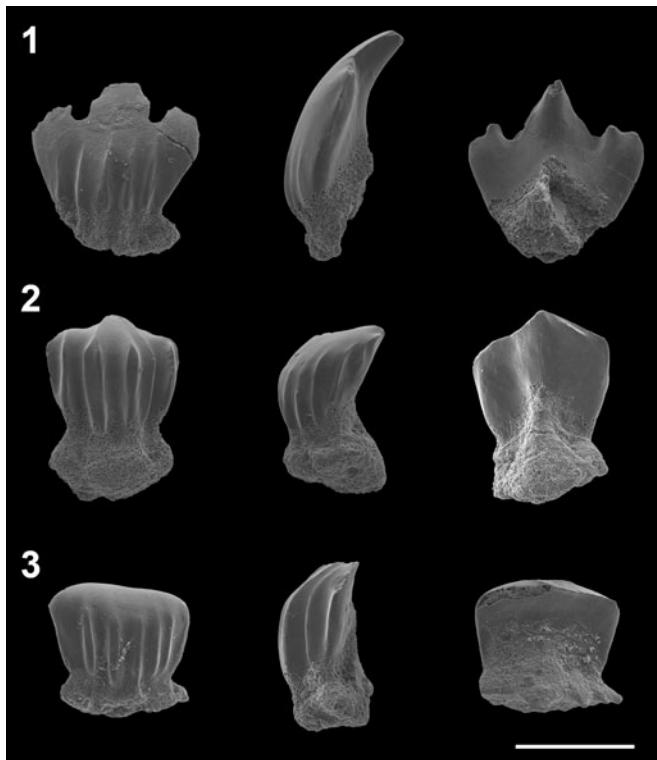


Figure 9. Placoid scales of *Cretodus crassidens* (Dixon, 1850), MPPSA IGVR 91032: (1) tricuspid placoid scale, in frontal, lateral, and posterior views; (2) single cusp placoid scale, in frontal, lateral, and posterior views; (3) rounded cusp placoid scale, in frontal, lateral, and posterior views. Scale bar = 500 μ m.

~25–53% of crown height, with the ratio increasing toward the distalmost rows.

Vertebral column.—MPPSA IGVR 91032 comprises only 86 vertebral centra, 51 on slab A and 35 on slab B. Measurements were provided by Amalfitano et al. (2017a, appendix B). Centra on slab A are partially articulated and represent the anterior part of the vertebral column (Figs. 3.1–3.2, 8.1). Centra on slab B are artificially aligned and decrease in size posteriorly (Figs. 3.1–3.2, 8.1). Vertebral centra are round, with height equal to width (Fig. 8.2). The sizes of the last centrum on slab A and the first centrum on slab B differ by ~20 mm, suggesting that a portion of the vertebral column between the two segments is missing (Amalfitano et al., 2017a). This is also indicated by the low vertebral count (86). The diameter of the centra on slab A ranges from 115 mm (vertebra 16) to 53 mm (vertebra 1); that on slab B ranges from 79 mm (first centrum of the slab) to 28 mm (last three centra) (Amalfitano et al., 2017a, appendix B). The mean length of the vertebral centra is $\sim 32.5 \pm 6.22$ mm (Amalfitano et al., 2017a, appendix B). The centra are well-calcified and structurally match the definition of ‘lamnoid vertebrae’ (sensu Applegate, 1967, p. 62; Fig. 8.2–8.4). Many centra of MPPSA IGVR 91032 suffer slight taphonomic distortion and some are incomplete, whereas a single one of BMB 007312 is nearly intact. The articular surface of the corpus calcareum is devoid of any kind of ornamentation and generally exhibits ~20 prominent concentric rings that are interpreted to be annual

incremental growth bands. These bands are not easily discernable on the vertebral centra of BMB 007312, probably due to erosion. In MPPSA IGVR 91032, a vertebral centrum deprived of the articular surface of the corpus calcareum due to biostratinomic processes (Fig. 8.3) presents concentric lamellae in the intermedialia and radial lamellae that are moderately thick (~1 mm). The radial lamellae tend to branch near the half of the radius length, enlarging and merging into composite and thick longitudinal septae toward the centrum periphery. The longitudinal septae, visible in lateral view in both MPPSA IGVR 91032 and BMB 007312 (Figs. 5.4, 8.4), are well-spaced with low density along the lateral surface of the centrum, separated by large fossae (~20 mm wide), except for the dorsal and ventral sides of the centrum, which exhibit a higher density of septae (three or four in an interval of ~20 mm). Diagonal or transverse septae are absent. Articular foramina are visible on some centra from MPPSA IGVR 91032 but are better visible on the complete vertebral centrum of BMB 007312, being more oval and larger than adjacent fossae (Figs. 5.4, 8.4).

Tessellated cartilage elements.—Seven main fragments of tessellated calcified cartilage are present on slab A of MPPSA IGVR 91032. Four occur close to each other at one extremity of the tooth accumulation and three are glued within the turtle remains. These tessellated cartilage elements probably split away from the slab during removal of the counterslab and have erroneously been glued to the turtle remains (Amalfitano et al., 2017a). The fragments are flat and range 55–130 mm in length and 40–85 mm in width. Their exposed surface shows the striated texture corresponding to the underlying polygonal prisms (tesserae; Dingerkus et al., 1991; Dean and Summers, 2006), which are well recognizable in the damaged areas. One of the fragments close to the tooth accumulation still has a lateral tooth associated (Fig. 3.3). The presence of a tooth rooted into one of the fragments further indicates that the fragment is part of the palatoquadrate or Meckel’s cartilage, possibly a commissural portion considering the tooth size.

Placoid scales.—Placoid scales (or dermal denticles) that covered the body of *Cretodus crassidens* are common in the reddish calcareous marly limestone embedding MPPSA IGVR 91032. They appear as whitish submillimetric prisms in the reddish rock. They are usually composed of a base, with a nutrient foramen at the bottom, and a crown (Fig. 9). The base is often missing because it is delicate and is easily damaged by the action of the acid used to dissolve the limestone to isolate them (Amalfitano et al., 2017a). Placoid scale height ranges 1–0.3 mm and width 0.6–0.3 mm. It was not possible to determine how the placoid scales were originally distributed. All scales are ornamented with strong parallel basoapical ridges and plications on the convex anterior face of their crown; ridges and plications do not extend posteriorly and have different sizes (from broad to slender) and general shapes (e.g., rhomboid, Fig. 9.1, 9.2; rounded or drop-like, Fig. 9.3). Except for some tricuspid scales (Fig. 9.1), the cusp is usually single, varying usually from pointed to rounded in shape (Fig. 9.2, 9.3).

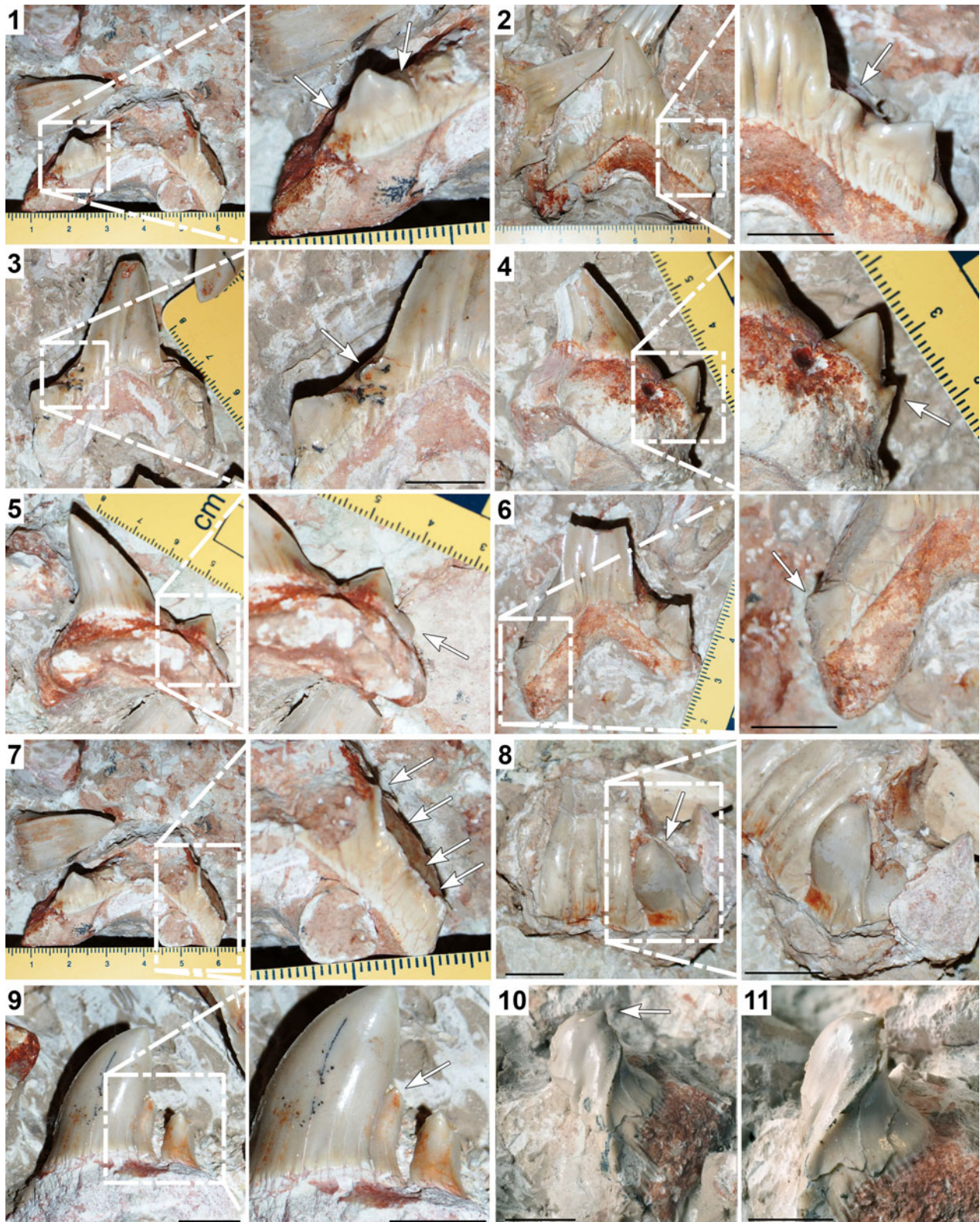


Figure 10. Variability in cusplet number and tooth malformations within the dentition of *Cretodus crassidens* (Dixon, 1850), MPPSA IGVR 91032: (1) tooth no. 10: the right shoulder of the central cusp has a crenulated cutting edge, whereas the other (arrows in detail view) bears a cusplet with two additional cusplules (a tricuspid cusplet); (2) tooth no. 24: the cutting edge between the main cusp and the cusplet has an accessory papilla (arrow in detail view); (3) tooth no. 33: cutting edge between the main cusp and the left cusplet has an accessory papilla (arrow in detail view); (4) tooth no. 35: smaller accessory cusplet occurs mesial to the mesial cusplet (arrow in detail view); (5) tooth no. 7: smaller accessory cusplet occurs mesial to the mesial cusplet (arrow in detail view); (6) tooth no. 32: left cusplet (arrow in detail view) is much smaller than the right cusplet; (7) tooth no. 10: right shoulder of the main cusp has an irregularly crenulated heel (the cusplet is absent; arrows in detail view), whereas the left shoulder has a cusplet with two additional cusplules (tricuspid cusplet); (8) tooth no. 47: the main cusp is bent lingually and the right cusplet is enlarged, bulky, and recurved lingually (arrow in main view; detail view is from the side); (9) tooth no. 58: right distal cusplet is enlarged and high; a distal slice of the main cusp grew independently and has its own apex (arrow in detail view); (10, 11) tooth no. 66 in labial and lateral view: the main cusp is partially twisted; its upper part is blunt and bears a diminutive and demarcated apex (arrow). Numbers matching those used by Amalfitano et al. (2017a, fig. 6). Scale bars = 10 mm.

Discussion

Taxonomy.—Genus-level taxonomy was recently commented upon by Siverson and Machalski (2017, p. 453, 454) and Shimada and Everhart (2019). The types of the first two described species of *Cretodus*—*Cretodus semiplicatus* (Münster in Agassiz, 1843) from the Turonian of Germany and *Cretodus crassidens* from the Turonian of the UK—are each based on isolated and poorly preserved teeth (Shimada and Everhart, 2019). The syntypes of *Cretodus semiplicatus* are considered marginally diagnostic for their poor preservation state and position (lateroposterior tooth, generally conservative in morphology among lamniforms and thus less taxonomically informative; Siverson and Machalski, 2017; Shimada and Everhart, 2019). Furthermore, being almost coeval, they could be conspecific with the type specimen of *Cretodus crassidens* (see Siverson and Machalski, 2017). Differences in morphology are addressed as dependent on different tooth position (syntype of *Cretodus semiplicatus* interpreted as a lower lateroposterior tooth, thus a more posterior position) and ontogenetic stage (Siverson and Machalski, 2017). The type specimen of *Cretodus crassidens*, a large, robust tooth with crenulated heels and lateral cusplet loss, might indicate a senile, female morphotype (Siverson and Machalski, 2017).

Shimada and Everhart (2019) clearly distinguished five species of the genus—*Cretodus crassidens*, *Cretodus giganteus* (Case, 2001), *Cretodus houghtonorum*, *Cretodus longiplicatus* Werner, 1989, and *Cretodus semiplicatus*—and proposed a phylogenetic hypothesis recognizing three categories based on similarities between the species ('*longiplicatus/semiplicatus*-grade,' '*giganteus/houghtonorum*-grade,' and '*crassidens*-grade'). Based on the original illustration of the holotype of *Cretodus sulcatus* (Geinitz, 1843), it is possible that *Cretodus longiplicatus* is a junior synonym of *Cretodus sulcatus* (see Siverson and Machalski, 2017). *Cretodus crassidens* is easily distinguished from its congeners by its mesiodistally broad teeth with large main cusp, robust lateral cusplets, and long vertical folds (to two-thirds of CH) and grooves on the labial face, especially in anteriormost rows. A rather large main cusp is also present in *Cretodus giganteus*, but this species seems to be more related to *Cretodus houghtonorum* for other characters and displays a thinner mesiodistal aspect (Shimada and Everhart, 2019). Basal crown 'costulae' (or 'striae'; Shimada and Everhart, 2019) are stronger and wider spaced than those of the '*giganteus/houghtonorum*-grade' (sensu Shimada and Everhart, 2019) but weaker and less dense than those of the '*semiplicatus/longiplicatus*-grade' (sensu Shimada and Everhart, 2019) and less evident in large teeth, but the difference is well recognizable in lateral teeth. Lateral cusplets of *Cretodus crassidens* also

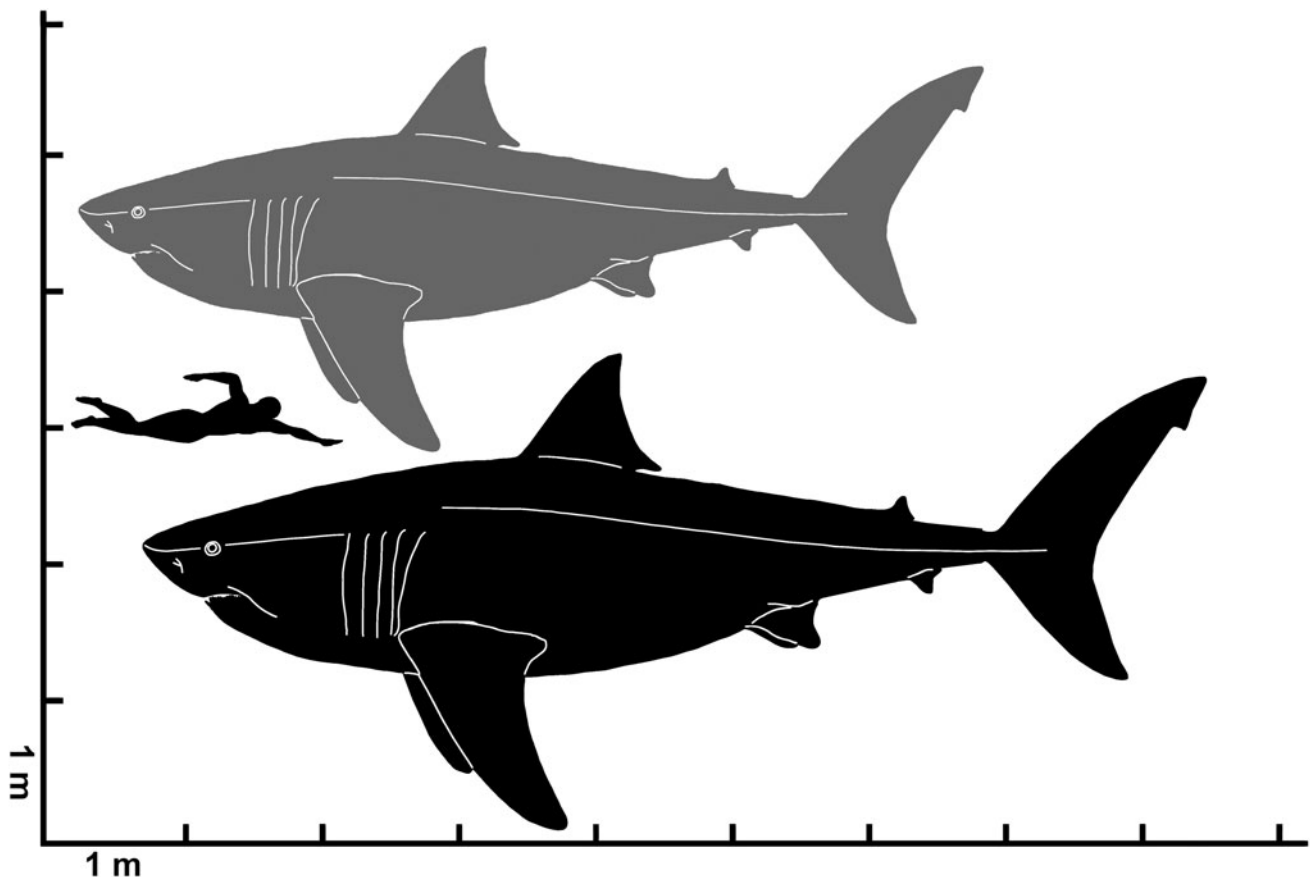


Figure 11. Estimated total length range for *Cretodus crassidens* (Dixon, 1850), MPPSA IGVR 91032. Gray silhouette indicates the lower limit (660 cm); black silhouette indicates the upper limit (780 cm). Silhouette modified after illustration by O.E. Demuth figured by Cooper et al. (2020, fig. 2D).

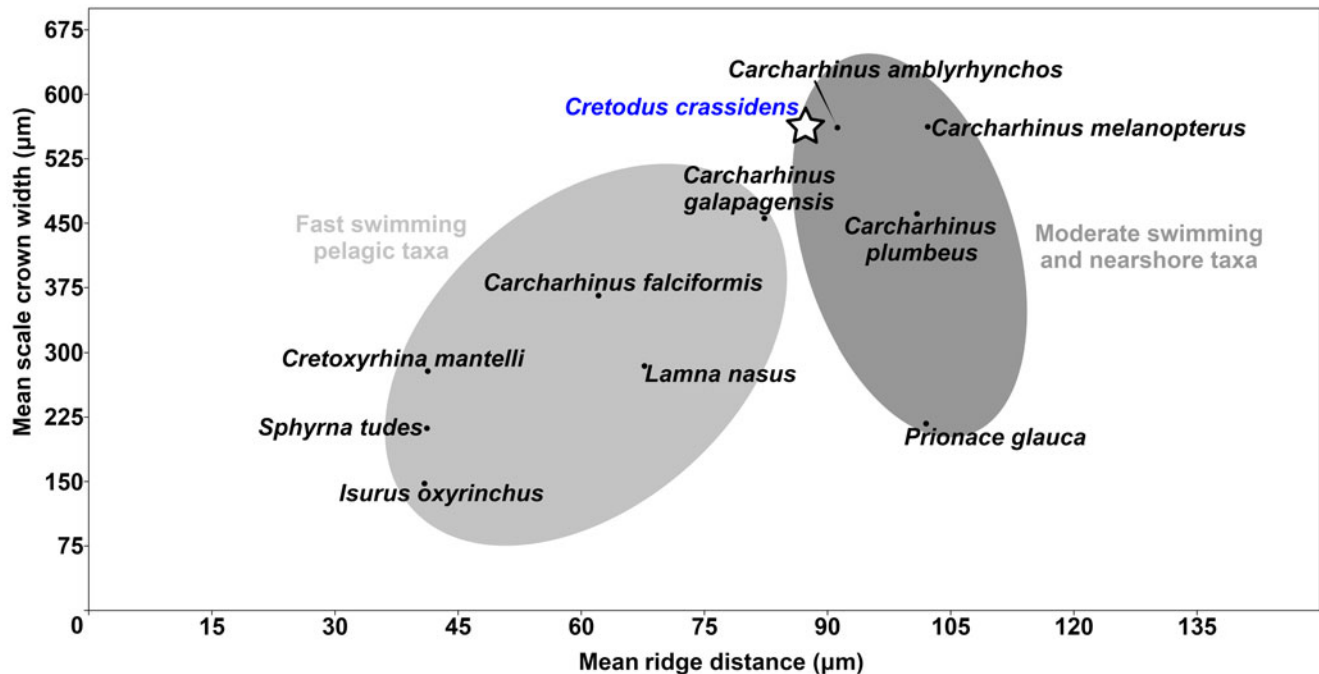


Figure 12. Correlation diagram of mean scale crown width (x axis) and mean ridge distance (y axis). Taxa in the light gray cloud are from the group of fast pelagic hunting sharks, whereas those in the dark gray cloud are from the group of large nearshore predators/moderate speed pelagic predators. Note that the *Cretodus crassidens* mean (star) falls within the cloud of correlation of large nearshore predators and moderate pelagic predators. Diagram modified after Reif (1985). Taxa not otherwise mentioned in the text include: *Carcharhinus amblyrhynchos* (Bleeker, 1856), *Carcharhinus falciformis* (Müller and Henle, 1841), *Carcharhinus galapagensis* (Snodgrass and Heller, 1905), *Carcharhinus melanopterus* (Quoy and Gaimard, 1824), *Carcharhinus plumbeus* (Nardo, 1827), *Isurus oxyrinchus* Rafinesque, 1810, *Lamna nasus* (Bonnaterre, 1788), *Prionace glauca* (Linnaeus, 1758), and *Sphyrna tudes* (Valenciennes, 1822).

differ from those of *Cretodus giganteus* by having a more robust aspect and divergent mesial and convergent distal cusplets, whereas both the cusplets of *Cretodus giganteus* are divergent (Shimada and Everhart, 2019).

The reconstruction of the dentition of *Cretodus crassidens* differs from that of the congeneric *Cretodus houghtonorum* in its mesiodistally broad morphology and strong vertical enameloid folds; the number of parasymphyseal teeth ('symphyseal' of Shimada and Everhart, 2019), three in the upper dentition and one in the lower one in *Cretodus houghtonorum*, two in both dentitions in *Cretodus crassidens*; and the presence of a reduced first upper anterior in *Cretodus crassidens*, although Shimada and Everhart (2019) interpreted it as an upper 'intermediate' (third upper anterior) tooth. The lateral teeth have similarly upright cusp, becoming more oblique distally, in both *Cretodus crassidens* and *Cretodus houghtonorum*. The number of lateral tooth rows is different: *Cretodus crassidens* has at least 10 upper laterals and eight lower laterals, whereas *Cretodus houghtonorum* has 11 upper laterals and eight lower laterals. Therefore, *Cretodus crassidens* has the following dental formula:

$$\frac{2P \ 3A \ 10(+2?)L}{2p \ 3a \ 8(+4?)l}$$

It must be noted that ontogenetic variation could strongly affect the taxonomy of *Cretodus*. Tooth size has been variously addressed as dependent on ontogenetic stage and dietary shifts during ontogeny, and care must be taken when using it as

taxonomic character (Adnet, 2006; Purdy and Francis, 2007; Belben et al., 2017; Marramà and Kriwet, 2017).

Comparing the dentition pattern presented herein with that of other Cretaceous lamniform sharks, the lack of specialized intermediate teeth combined with the presence of at least one upper parasymphyseal file is commonly found in Cretaceous taxa other than *Cretodus* (e.g., *Archaeolamna* Silversson, 1992, *Cardabiodon* Silversson, 1999, *Cretalamna* Glickman, 1958, *Cretoxyrhina* Glickman, 1958, *Haimrichia* Vullo, Guinot, and Barbe, 2016; Shimada, 1997c, 2007; Siverson, 1999; Cook et al., 2011; Dickerson et al., 2013; Silversson et al., 2013, 2015; Vullo et al., 2016). The presence of a reduced first upper anterior has been reported in other Cretaceous and modern lamniforms (e.g., *Alopias* Rafinesque, 1810, *Carcharias* Rafinesque, 1810, *Cardabiodon*, *Haimrichia*, *Odontaspis* Agassiz, 1838; Applegate, 1965; Shimada, 2002; Siverson, 1999; Vullo et al., 2016).

Vertebral centra are considered poor in diagnostic characters in lamniforms, except for a few cases in which their morphology has been observed in detail (e.g., Newbrey et al., 2015). Comparing vertebral centrum morphology in *Cretodus* with that of other neoselachians (Newbrey et al., 2015), *Cretodus* is characterized by distinctive radial lamellae branching and organizing in composite and thick septae toward the periphery of the centrum, divided by large fossae. These structures are different from those observed in other extant and extinct lamniform sharks and could represent a genus- or family-level diagnostic character. However, a family-level taxonomic discussion is well beyond the scope of this paper and needs further evidence

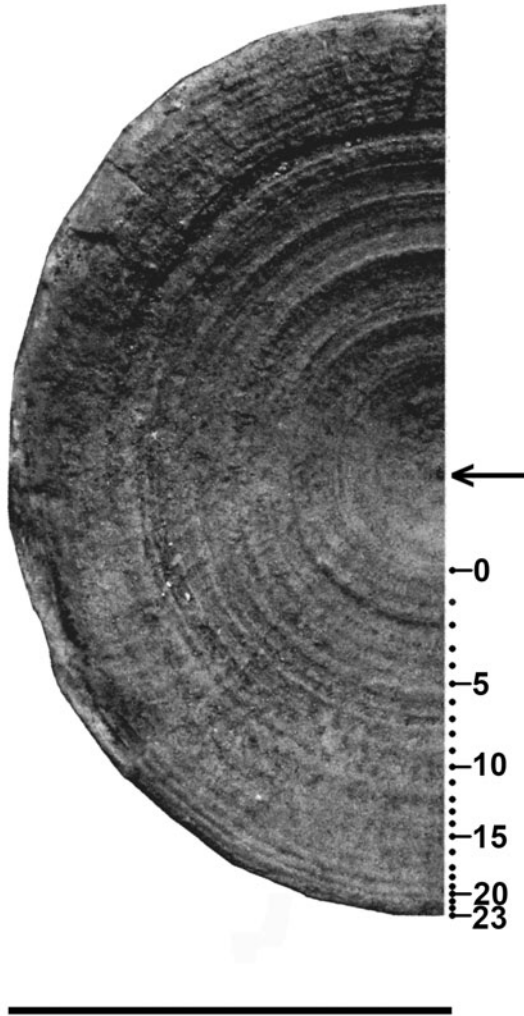


Figure 13. Growth band pairs count of *Cretodus crassidens* (Dixon, 1850), MPPSA IGVR 91032. Vertebral centrum shows 23 incremental growth band pairs presumably formed annually (arrow indicates the center of the centrum; '0' indicates vertebral size at birth). Scale bar = 50 mm.

from additional complete or associated remains of closely related genera.

Teratologic remarks.—A certain variability in the morphological pattern of the cusplets that could be interpreted as malformations (Gudger, 1937; Becker et al., 2000) can be observed in MPPSA IGVR 91032 (Figs. 10, 11; Amalfitano et al., 2017a, fig. 6). In tooth number 10, one of the shoulders of the central cusp bears a cusplet with two further cuspules, i.e., a tricuspid cusplet (Fig. 10.1). The other shoulder has a crenulated cutting edge (Fig. 10.1). In three teeth (nos. 22, 24, and 33), a papilla is present on the cutting edge between the central cusp and the normally developed cusplet. In two cases (nos. 24 and 33; Fig. 10.2, 10.3), this occurs in the mesial half of the crown. A small supplementary cusplet is found in three teeth (nos. 2, 7, and 35; Fig. 10.4, 10.5) mesial to the mesial cusplet. In another tooth (no. 9), it is unclear whether the small supplementary cusplet is mesial to the mesial cusplet or distal to the distal

cusplet. In two cases (nos. 2 and 35), it is triangular in outline and pointed, whereas in others it is papilla-like. In one tooth (no. 32; Fig. 10.6), one cusplet (the distal one) is smaller than the other.

Besides those with additional or smaller cusplets, the sample also contains malformed teeth (Fig. 10.7–10.11). Tooth number 10 has a weakly and irregularly crenulated heel on the shoulder of the main cusp instead of a well-formed cusplet (Fig. 10.7). This kind of malformation also occurs in three other teeth (nos. 52, 81, and 96). The main cusp of tooth number 47 (Fig. 10.8) is bent lingually and one cusplet is overgrown, bulky, and also recurved lingually. Tooth number 58 (Fig. 10.9) has the central cusp divided into two parts by a deep notch; the distal slice grew independently with its own apex, like a shark tooth figured by Welton and Farish (1993, fig. 17K). Furthermore, the distal cusplet is overgrown and tall. Tooth number 66 (Fig. 10.10, 10.11) has a main cusp that is partially twisted, and its apical part is blunt with a demarcated, diminutive apex.

Malformed teeth also occur in other *Cretodus crassidens* specimens from the Chalk Group of England discussed herein. The most common malformation is the loss of lateral cusplet and replacement by a weakly, irregularly crenulated heel on the shoulder of the main cusp. This kind of malformed tooth is present in specimens with associated tooth sets, e.g., NHMUK PV OR 25786 and BMB 007312, but also in isolated teeth, namely the holotype NHMUK PV OR 25823, NHMUK PV OR 49951, and NHMUK PV P 12870.

Malformed teeth have been object of several studies and reports on both fossil and living sharks. Gudger (1937) provided the probably first methodic report of malformed teeth in extant sharks. Later, some authors focused on tooth pattern reversal (Compagno, 1967; Reif, 1980), which also contributed to the development of subsequent studies on pattern formation in development of chondrichthyan dentitions from an evolutionary perspective (Smith et al., 2013). Other studies focused on feeding-related malformations in early growth stages (Becker et al., 2000; Becker and Chamberlain, 2012). Tooth anomalies in fossil and extant sharks consist mainly of curved or twisted crowns, punctures or notches, deformed or missing cusps, fusion of teeth of the same tooth family, excessive growth of dentine, or abnormal root morphology (Becker et al., 2000; Witzmann et al., 2021). Because damaged shark teeth cannot heal, Johnson (1987) and Welton and Farish (1993) regarded all shark tooth deformities as developmental in origin, i.e., the result of mutation or damage at an early growth stage (Witzmann et al., 2021). Based on comparisons with extant sharks, Becker et al. (2000) noted that many of the observed tooth anomalies in extant and fossil sharks were likely from feeding-related injury to the dental lamina of the jaws, particularly by impaction of chondrichthyan and teleost fin and tail spines. Furthermore, these authors explicitly stated that at least some malformed teeth could be caused by disease or mutation. However, the original cause of any dental anomaly could be virtually impossible to determine in a fossil shark (Shimada, 1997c; Witzmann et al., 2021).

Teeth of the sample described above are affected by several malformations that do not differ from malformations listed above and reported in other sharks. Fifteen teeth out of 120 total (including those with atypical size or number of cusplets)

exhibit malformations. Despite the incompleteness of the sample, the incidence of malformations in only one specimen is rather high, if compared with other Cretaceous species numbers with larger datasets (e.g., from ~0.015% in *Squalicorax kaupi* (Agassiz, 1843) to ~0.36% in *Paranomotodon* sp.; Becker et al., 2000). This difference is certainly due to a sampling bias, but the high incidence could be due to the peculiar trophic preferences of *Cretodus crassidens*, as evidenced by the association with marine turtle remains, or to the ontogenetic stage of the individual. Thus, the dental malformations could be interpreted as feeding-related injuries to the dental lamina (e.g., Becker et al., 2000) or as senile characters (especially the lateral cusplet loss and replacement with crenulated heel; Siverson and Machalski, 2017).

Body size and body form: paleoecological remarks.—The Italian specimen MPPSA IGVR 91032 allows some suppositions on the overall morphology and size of *Cretodus crassidens*. The two segments preserved measure ~244 cm and 182 cm (although the latter was completely reworked by the preparator). The sum is ~426 cm, but many vertebral centra are missing and this could be an underestimation of the TL of the individual. Applying the least square linear regression method (Supplemental Data 1; $r^2 = 0.86115$), it is possible to estimate an original vertebral count of 169 vertebral centra, similar to the vertebral count of other extant and extinct large lamniform sharks (Springer and Garrick, 1964; Shimada et al., 2006; Natanson et al., 2018). The mean length of the vertebral centra is $\sim 32.5 \pm 6.22$ mm, therefore the estimated articulated vertebral column is ~549 cm long. Considering the intervertebral disc length (+10%; Newbrey et al., 2015), taphonomic compression (+20%; Newbrey et al., 2015), and skull length (+50 cm; approximation based on the *Cretoxyrhina* skull length, 60 cm, from Shimada, 1997c and Newbrey et al., 2015, and presuming a shorter and more laterally expanded skull in *Cretodus*), the estimated total length of the Italian specimen is ~764 cm. The body size estimates reported by Amalfitano et al. (2017a) suggested a TL ranging 661–776 cm based on the size of the vertebral centra. The new estimate, based on the vertebral centrum length and approximate vertebral count, falls within the previous estimated range. This estimate can be compared also to TL estimates based on tooth size. The largest CH measured in the Italian specimen is ~56 mm (Appendix 1) and if the CH of 56 mm is applied to the equation used by Shimada (2008), the calculation provides a TL of 700 cm. On the other hand, the linear function from Shimada et al. (2020) provides an estimated TL of ~659.6 cm, which, if applied to the largest teeth of the *Cretodus crassidens* dentition, is very close to the previous value of 661 cm based on vertebral centra diameter. Shimada and Everhart (2019) also suggested that *Cretodus* had a stouter body than *Cretoxyrhina*, observing the arrangement of the teeth in a 120 cm wide arch (assuming that they are not dislodged) and the 156 cm long, 108 cm wide elliptical accumulation of turtle bones interpreted as gastric content. These indicate a rather stout body, with an abdominal width of at least 108 cm, and a wide, gently curved, laterally expanded mouth aperture, almost semielliptical, more like *Galeocerdo* Müller and Henle, 1837 (Randall, 1992) or,

compared to any other lamniform shark, *Squalicorax* Whitley, 1939 (Shimada and Cicimurri, 2005). Accordingly, the head would also be laterally expanded. The shape of vertebral centra, almost perfectly circular and rostrocaudally short, is like many other Cretaceous lamniform sharks (e.g., *Cretoxyrhina*, Shimada, 1997c; *Cardabiodon*, Newbrey et al., 2015; *Squalicorax*, Shimada and Cicimurri, 2005). Thus, it could be inferred that this shark had a fusiform body with a circular girth at the trunk region, with a great vertebral column elasticity that allowed carangiform swimming behavior (Newbrey et al., 2015). The length of the entire semielliptical dental arch, calculated with a geometric approximation (Supplemental Data 2), is ~137 cm. Using, then, this new value applied to the relation between ‘bite circumference’ and TL by Lowry et al. (2009), the estimated TL of the individual is ~813 cm. All of these estimates are more or less consistent, and it is reasonable to define an estimated range of TL between ~660 and ~780 cm (Fig. 11), based on the vertebral centrum diameter, which is apparently the least biased proxy.

Another parameter useful to infer body form and paleoecology of a shark is the morphology of the placoid scales (Reif, 1982, 1985; Reif and Dinkelacker, 1982), which are preserved in MPPSA IGVR 91032. Amalfitano et al. (2017a) and Shimada and Everhart (2019) discussed the morphology of the placoid scales to infer the swimming behavior of *Cretodus*. Shimada and Everhart (2019) observed, contra Amalfitano et al. (2017a), that the strong ridges and plications ornamenting the placoid scale crown do not extend posteriorly on the exterior crown face, unlike those of typical fast-swimming lamniforms, including fossil taxa interpreted as fast pelagic-hunting sharks, e.g., *Cretoxyrhina* (Shimada, 1997b, c; Shimada et al., 2006; Amalfitano et al., 2019) and *Cardabiodon* (Dickerson et al., 2013; Newbrey et al., 2015). This morphological condition is also present in scales of the holotype of *Cretodus houghtonoum* (FHSM VP 17575; Shimada and Everhart, 2019). For this reason, the ridge spacing and the crown width from the original sample of Amalfitano et al. (2017a) were measured (Appendix 3). The mean scale crown width is 562 ± 103.31 μm , whereas the mean ridge spacing is 87.32 ± 30.65 μm . Plotting these values with those of extant sharks and *Cretoxyrhina mantelli* Agassiz, 1835 (data retrieved from Reif, 1985, Shimada, 1997a, and Amalfitano et al., 2019; Fig. 12), the *Cretodus crassidens* value falls close to the group of large nearshore predators and moderate-speed pelagic predators (sensu Reif, 1985). This confirms the assumption made by Shimada and Everhart (2019) that considers *Cretodus* a more sluggish swimmer with higher maneuverability (as also evidenced by vertebral centra morphology) than thunniform fast-cruising swimmers, e.g., *Cretoxyrhina*. This assumption is corroborated by association with the turtle remains, which suggests a trophic preference of *Cretodus crassidens* toward these reptiles, similar to that of the extant tiger shark, *Galeocerdo cuvier* (Péron and Lesueur in Lesueur, 1922), which displays very similar placoid scale ornamentation combined with the ecological niche of a large nearshore predator (Reif, 1985). Shimada and Everhart (2019), in their discussion of the ecology of the genus *Cretodus*, reported that during excavation of the holotype of *Cretodus houghtonoum* (FHSM VP 17575) that remains of two additional species of sharks were identified from the same stratigraphic

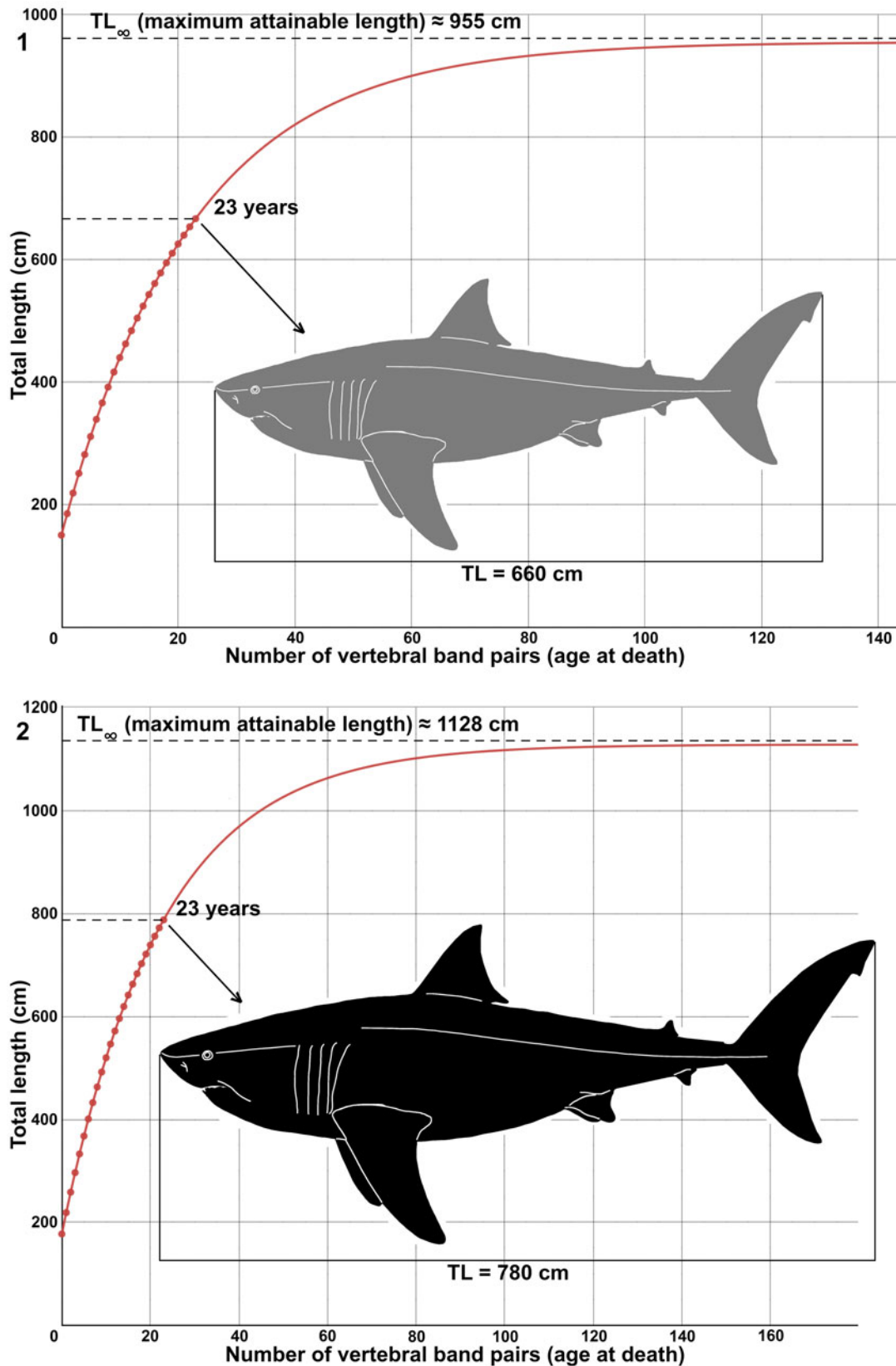


Figure 14. Suggested growth models of *Cretodus crassidens* (Dixon, 1850) based on MPPSA IGVR 91032 (see text; Table 1): (1) von Bertalanffy growth function fitted to data points that show the relationship of number of vertebral growth band pairs with estimated total body length of 660 cm (TL_1); (2) von Bertalanffy growth function fitted to data points that show relationship of number of vertebral growth band pairs with estimated total body length of 780 cm (TL_2). Gray silhouette indicates the lower limit (660 cm); black silhouette indicates the upper limit (780 cm). Silhouette modified after illustration by O.E. Demuth figured by Cooper et al. (2020, fig. 2D).

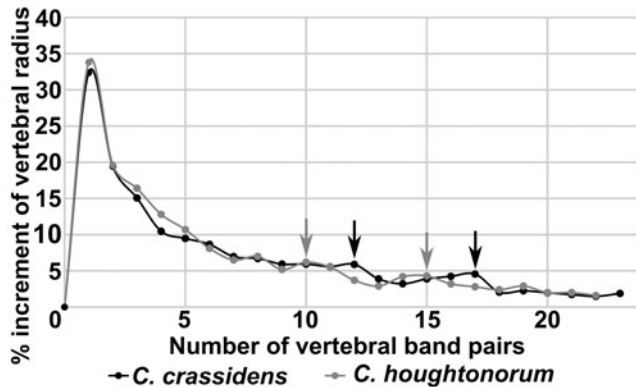


Figure 15. Plot of percentage increment of the vertebral radius of *Cretodus crassidens* (Dixon, 1850) (MPPSA IGVR 91032) and *Cretodus houghtonorum* Shimada and Everhart, 2019 (FHSM VP 17575). Arrows indicate peaks interpreted as maturity onset for *Cretodus crassidens* (black) and *Cretodus houghtonorum* (gray).

horizon in immediate association with FHSM VP 17575, namely two teeth of *Squalicorax* cf. *S. falcatus* (Agassiz, 1843) (FHSM VP 19273 and 19274) and two partial dorsal fin spines of a hybodontid shark (FHSM VP 19272) comingled with remains of *Cretodus houghtonorum*. This fossil association is interpreted as another case of a ‘vertebrate three-level trophic chain’ (Kriwet et al., 2008, p. 183), but involving three species of sharks in this instance (Shimada and Everhart, 2019). The individual of *Cretodus houghtonorum* must have died shortly after ingesting the hybodont because of the absence of acid-etching alteration on the hybodont remains; the *Cretodus houghtonorum* carcass was scavenged by *S. cf. S. falcatus* before or during the decay, followed by disarticulation and scattering of the skeletal and dental elements of *Cretodus houghtonorum* due to the presence of weak water currents on the seafloor (Shimada and Everhart, 2019). Hybodont remains are more common in shallow-nearshore environments, if not in fresh or brackish water environments (e.g., Underwood and Rees, 2002; Underwood, 2004; Sweetman and Underwood, 2006), and the presumed predator-prey relationship between *Cretodus houghtonorum* and the hybodontid shark suggests that *Cretodus houghtonorum* dwelled, at least sometimes, in shallow-nearshore environments. This assumption is supported by the fact that although *Cretodus houghtonorum* and *Cretoxyrhina mantelli* lived contemporaneously (Shimada, 2006), the distribution of the two taxa indicates that they likely practiced resource partitioning within the North American Western Interior Sea, because *Cretodus houghtonorum* teeth are more commonly found in nearshore deposits whereas those of *Cretoxyrhina mantelli* are common in offshore deposits (Shimada and Everhart, 2019). The occurrence of *Cretodus crassidens* in the pelagic deposits of the Scaglia Rossa and Chalk Group, however, implies that this species preferentially dwelled in the offshore setting. It must be remarked, however, that *Cretodus crassidens* is represented by a single specimen in the Scaglia Rossa to date, whereas *Cretoxyrhina mantelli* and *Ptychodus* spp. remains are much more common (Amadori et al., 2019, 2020a, b; Amalfitano et al., 2019).

Age estimate and growth model.—One of the vertebral centra of MPPSA IGVR 91032 exhibits a total of 23 pairs of growth bands on the articular surface of the corpus calcareum (Fig. 13, Table 1). Each pair of growth bands is traditionally interpreted to have been deposited annually (Cailliet, 1990; Cailliet and Goldman, 2004), with the total band pair number (BN) indicating the age at death. Such growth band pairs do not necessarily record age or time but rather are related simply to growth or vertebral size (Harry, 2018; Natanson et al., 2018; Natanson and Deacy, 2019). Hence, the relationship of BN with time or age is loosely correlated (Natanson et al., 2018) and generally tends to retrieve an underestimation or an overestimation, because not all growth bands are necessarily consistent with aging for the entire lifespan (Passerotti et al., 2014; Harry, 2018; Natanson et al., 2018), especially in older individuals or when later growth bands are not annual. However, it is possible to hypothesize that the individual of *Cretodus crassidens* MPPSA IGVR 91032 was at least 23 years old at the time of its death if the deposition of each pair of growth bands is annual. The hypothetical von Bertalanffy growth function (VBGF) is here reconstructed based on the individual MPPSA IGVR 91032 and following the same estimates made by Shimada and Everhart (2019), with the aim to compare the ontogenetic growth of the two species *Cretodus crassidens* and *Cretodus houghtonorum* (Figs. 14, 15). The VBGF is applied to the size estimates discussed above, namely ~660 cm and ~780 cm. The VBGF fitted to the BN-TL (660 cm) (Fig. 14.1) data gives the following growth parameter estimates: L_{∞} (maximum TL) = 955.22 cm; L_0 (total length at birth) = 141.9 cm; $k = 0.045 \text{ yr}^{-1}$; estimated longevity (after Natanson et al., 2006) = 64.429 yr. The BN-TL (780 cm) data (Fig. 14.2), on the other hand, retrieve the following parameters: $L_{\infty} = 1128.8 \text{ cm}$; $L_0 = 167.7 \text{ cm}$. The longevity estimate of ~64 yr is consistent with those for extant large lamniform sharks (Camhi et al., 2008) and that of *Cretodus houghtonorum* (~55 years; Shimada and Everhart, 2019).

The percentage increment of the centrum radius of *Cretodus crassidens* and *Cretodus houghtonorum* was also considered to find any significant variation in growth rate and for further comparison (Fig. 15). The percentage increment of the two species is almost identical, except for two delayed peaks, which could correspond to the maturity onset at 12–17 years and 10–15 years, respectively. The maturity onset is consistent with those of other large macropredatory lamniform sharks (Camhi et al., 2008). The delayed growth peaks could alternatively be caused by sexual dimorphism, with females maturing later than males (Camhi et al., 2008). However, despite the strong similarities between the two species, there is no evidence to support *Cretodus crassidens* and *Cretodus houghtonorum* identifications as gynandric heterodont variants, but rather they were vicariant species dwelling in different environments (*Cretodus crassidens* in offshore settings, *Cretodus houghtonorum* in nearshore settings) or geographically separated (*Cretodus crassidens* in the European Tethys and Boreal seas, *Cretodus houghtonorum* in the Western Interior Seaway; see also Guinot and Cavin, 2016 for vicariations related to the Cenomanian diversification event). After attaining maturity, the growth rate

in the plot generally tends to become asymptotic, as evidenced after the peaks at 17 and 15 yr, respectively.

The growth model provided herein allows calculation of the possible TL of other specimens. The growth bands are not well preserved on the two vertebral centra of BMB 007312. The specimen also includes the lower second anterior tooth, the CH of which measures 47 mm (Appendix B). If the linear functions CH-TL extrapolated from MPPSA IGVR 91032 is applied, i.e.,

$$TL_1(\text{cm}) = 11.78 \times \text{CH}(\text{mm}) + 0.24 \quad (4)$$

$$TL_2(\text{cm}) = 13.92 \times \text{CH}(\text{mm}) + 0.29 \quad (5)$$

the estimated TL of BMB 007312 results in a range between ~554 cm and ~654 cm (versus an estimated TL range of 546–573 cm when applying the equations used by Amalfitano et al. [2017a] based on vertebral centrum diameter). The age at death was ~16–17 years if the CH is considered, comparing this specimen to MPPSA IGVR 91032 (Table 1).

Conclusions

The specimen MPPSA IGVR 91032 and others described herein provide new morphological and paleobiological information about the Late Cretaceous large-sized shark genus *Cretodus*. The specimen is assigned to *Cretodus crassidens* and reconstruction of its dentition based on the Italian specimen reveals the peculiarities of this species with respect to other species of the genus. *Cretodus crassidens* likely represents a separate lineage within *Cretodus* (see the phylogenetic hypothesis by Shimada and Everhart, 2019). The body form and size estimates are indicative of a large-sized macropredatory shark, reaching a size over the limit that defines gigantic elasmobranch species (> 6 m; Pimiento et al., 2019). The maximum estimated total length (9–11 m) and length at birth are comparable to those of the giant Cenozoic genus *Otodus* Agassiz, 1838 (Shimada et al., 2021). *Cretodus crassidens* was probably characterized by a moderate-speed swimming behavior, suggested by the morphology of the vertebral centra and the placoid scales. This shark was a large predator feeding on, among others, large protostegid turtles, as evidenced by the gastric content preserved within the individual from the basinal high settings of the ‘Lastame.’ Estimated age at death (23 yr) and longevity (64 yr) are consistent with those of extant large lamniform shark populations not subject to anthropic pressure. Interestingly, this study notes that *Cretodus crassidens* fossils occur both in Boreal and Tethyan domains at the same interval, implying a broad paleobiogeographic distribution. Moreover, *Cretodus crassidens* exhibits a likely preference toward offshore settings, in contrast with other species of the genus found in nearshore settings, indicating a possible vicariance scenario. Another conceivable hypothesis could be age- (thus size-) related partitioning with very large individuals less suited to hunt in nearshore environments; however, further evidence is required to fully resolve that scenario.

Acknowledgments

R. Zorzin (Museo Civico di Storia Naturale di Verona), E. Bernard (NHMUK), and L. Ismail and J. Cooper (BMB) are deeply thanked for access to the specimens and to information about the collections under their care. Copyright of the NHMUK photos is reserved by K. Webb and The Natural History Museum (NHMUK). S. Castelli (Dipartimento di Geoscienze, Università degli Studi di Padova) is also acknowledged for their valuable contribution with photos and postproduction for the Italian material. Funding for this research was provided by University of Padova (Progetto di Ateneo CPDA159701/2015, titled ‘Reappraisal of two key Fossil-Lagerstätten in Scaglia deposits of northeastern Italy in the context of Late Cretaceous climatic variability: a multidisciplinary approach,’ assigned to E. Fornaciari and Dotazione Ordinaria Ricerca (DOR) funds assigned to L. Giusberti). The reviewers M. Siversson, C. Underwood, and D.J. Ward, and the Editor H.-D. Sues are deeply thanked for helpful and valuable suggestions on an earlier draft of this paper.

Data availability statement

Data available from the Dryad Digital Repository: <https://doi.org/10.5061/dryad.31zcrjdnk>.

References

- Adnet, S., 2006, Biometric analysis of the teeth of fossil and Recent hexanchid sharks and its taxonomic implications: Acta Palaeontologica Polonica, v. 51, no. 3, p. 477–488.
- Agassiz, L.J.R., 1835, Rapport sur les Poissons Fossiles Découverts Depuis la Publication de la Troisième Livraison, Feuilleton Additionnel sur les Recherches sur les Poissons Fossiles, 4th Livraison: Neuchâtel, Switzerland, Petitpierre et Prince, p. 39–64.
- Agassiz, L.J.R., 1838, Recherches sur les Poissons Fossiles, 11th Livraison: Neuchâtel, Switzerland, Petitpierre et Prince (text) and H. Nicolet (plates), v. 2, pls. 42, 43; v. 3, p. [73]–140, pls. 1a, 8a, 8b, 15, 17, 19, 20, 24, 25b, 30–35, 39, 40; v. 5, pl. 60; Feuilleton Additionnel, p. 107–116.
- Agassiz, L.J.R., 1843, Recherches sur les Poissons Fossiles, 15th and 16th Livraisons: Soleure, Switzerland, Jent and Gassmann (text), and Neuchâtel, Switzerland, H. Nicolet (planches), v. 2, pt. 2, p. [1]–72, pls. B*, B**, Ca, G, 23b, 23c, 31, 33a, 36–38, 42a, 44; v. 3, p. 157–390, 382*–382**, 1–32, [33]–[34], pls. 1, 18, 22, 22a, 22b, 26a, 38, 40b–40d, 45, 47; vol. 4, pl. 23b; vol. 5, pt. 2, p. 57–84, pls. B, C, E, H, J, K, 9, 10, 28, 29, 37b, 44–48; Feuilleton Additionnel, p. 139–144.
- Amadori, M., Amalfitano, J., Giusberti, L., Fornaciari, E., Luciani, V., Carnevale, G., and Kriwet, J., 2019, First associated tooth set of a high-cusped *Ptychodus* (Chondrichthyes, Elasmobranchii) from the Upper Cretaceous of northeastern Italy, and resurrection of *Ptychodus altior* Agassiz, 1835: Cretaceous Research, v. 93, p. 330–345, <https://doi.org/10.1016/j.cretres.2018.10.002>.
- Amadori, M., Amalfitano, J., Giusberti, L., Fornaciari, E., Carnevale, G., and Kriwet, J., 2020a, The Italian record of the Cretaceous shark, *Ptychodus latissimus* Agassiz, 1835 (Chondrichthyes; Elasmobranchii): PeerJ, v. 8, p. e10167, <https://doi.org/10.7717/peerj.10167>.
- Amadori, M., Amalfitano, J., Giusberti, L., Fornaciari, E., Carnevale, G., and Kriwet, J., 2020b, A revision of the Upper Cretaceous shark *Ptychodus mediterraneus* Canavari, 1916 from northeastern Italy, with a reassessment of *P. latissimus* and *P. polygyrus* Agassiz, 1835 (Chondrichthyes; Elasmobranchii): Cretaceous Research, v. 110, p. 104386, <https://doi.org/10.1016/j.cretres.2020.104386>.
- Amalfitano, J., Dalla Vecchia, F.M., Giusberti, L., Fornaciari, E., Luciani, V., and Roghi, G., 2017a, Direct evidence of trophic interaction between a large lamniform shark, *Cretodus* sp., and a marine turtle from the Cretaceous of northeastern Italy: Palaeogeography, Palaeoclimatology, Palaeoecology, v. 469, p. 104–121, <https://doi.org/10.1016/j.palaeo.2016.12.044>.
- Amalfitano, J., Giusberti, L., Dalla Vecchia, F.M., and Kriwet, J., 2017b, First skeletal remains of the giant sawfish *Onchosaurus* (Neoselachii,

- Shimada, K., Cumba, S.L., and van Rooyen, D., 2006, Caudal fin skeleton of the Late Cretaceous shark, *Cretoxyrhina mantelli* (Lamniformes: Cretoxyrhinidae) from the Niobrara Chalk of Kansas: Bulletin of New Mexico Museum of Natural History, v. 35, p. 185–192.
- Shimada, K., Becker, M.A., and Griffiths, M.L., 2020, Body, jaw, and dentition lengths of macrophagous lamniform sharks, and body size evolution in Lamniformes with special reference to ‘off-the-scale’ gigantism of the megatooth shark, *Otodus megalodon*: Historical Biology, v. 33, no. 11, p. 2543–2559, <https://doi.org/10.1080/08912963.2020.1812598>.
- Shimada, K., Bonnan, M.F., Becker, M.A., and Griffiths, M.L., 2021, Ontogenetic growth pattern of the extinct megatooth shark *Otodus megalodon*—Implications for its reproductive biology, development, and life expectancy: Historical Biology, v. 33, no. 12, p. 3254–3259, <https://doi.org/10.1080/08912963.2020.1861608>.
- Siverson, M., 1992, Biology, dental morphology and taxonomy of lamniform sharks from the Campanian of the Kristianstad Basin, Sweden: Palaeontology, v. 35, p. 519–554.
- Siverson, M., 1999, A new large lamniform shark from the uppermost Gearle Siltstone (Cenomanian, Late Cretaceous) of Western Australia: Earth and Environmental Science Transactions of the Royal Society of Edinburgh, v. 90, no. 1, p. 49–66.
- Siverson, M., and Machalski, M., 2017, Late late Albian (Early Cretaceous) shark teeth from Annapol, Poland: Alcheringa: An Australasian Journal of Palaeontology, v. 41, no. 4, p. 433–463, <https://doi.org/10.1080/03115518.2017.1282981>.
- Siverson, M., Lindgren, J., and Kelley, L.S., 2007, Anacoracid sharks from the Albian (Lower Cretaceous) Pawpaw Shale of Texas: Palaeontology, v. 50, no. 4, p. 939–950, <https://doi.org/10.1111/j.1475-4983.2007.00691.x>.
- Siverson, M., Ward, D.J., Lindgren, J., and Kelley, L.S., 2013, Mid-Cretaceous *Cretoxyrhina* (Elasmobranchii) from Mangyshlak, Kazakhstan and Texas, USA: Alcheringa: An Australasian Journal of Palaeontology, v. 37, no. 1, p. 87–104, <https://doi.org/10.1080/03115518.2012.709440>.
- Siverson, M., Lindgren, J., Newbrey, M.G., Cederström, P., and Cook, T.D., 2015, Cenomanian–Campanian (Late Cretaceous) mid-palaeolatitude sharks of *Cretalamna appendiculata* type: Acta Palaeontologica Polonica, v. 60, p. 339–384, <https://doi.org/10.4202/app.2012.0137>.
- Smith, M.M., Johanson, Z., Underwood, C., and Diekwisch, T.G., 2013, Pattern formation in development of chondrichthyan dentitions: A review of an evolutionary model: Historical Biology, v. 25, no. 2, p. 127–142, <https://doi.org/10.1080/08912963.2012.662228>.
- Snodgrass, R.E., and Heller, E., 1905, Papers from the Hopkins-Stanford Galapagos Expedition, 1898–1899, 17, Shore fishes of the Revillagigedo, Cliperton, Cocos and Galapagos islands: Proceedings of the Washington Academy of Sciences, v. 6, p. 333–427.
- Springer, V.G., and Garrick, J.A.F., 1964, A survey of vertebral numbers in sharks: United States National Museum Proceedings, v. 116, p. 73–96.
- Sokolov, M.I., 1965, Evolyutsiya zubov nekotorykh rodov melovykh akul i rekonstruktsiya ikh ozubleniya [Teeth evolution of some genera of Cretaceous sharks and reconstruction of their dentition]: Byulleten’ Moskovskogo Obshchestva Ispytateley Prirody, n.s., v. 70, Otdel Geologicheskii, v. 40, no. 4, p. 133–134. [in Russian]
- Sweetman, S.C., and Underwood, C.J., 2006, A neoselachian shark from the non-marine Wessex Formation (Wealden Group: Early Cretaceous, Barremian) of the Isle of Wight, southern England: Palaeontology, v. 49, no. 2, p. 457–465, <https://doi.org/10.1111/j.1475-4983.2006.00549.x>.
- Trevisani, E., and Cestari, R., 2007, Upper Cretaceous bivalves from basinal highs (Venetian Prealps, northern Italy), in Scott, R.W., ed., Cretaceous Rudists and Carbonate Platforms: Environmental Feedback: SEPM Special Publications, v. 87, p. 71–80.
- Underwood, C.J., 2004, Environmental controls on the distribution of neoselachian sharks and rays within the British Bathonian (Middle Jurassic): Palaeogeography, Palaeoclimatology, Palaeoecology, v. 203, no. 1/2, p. 107–126, [https://doi.org/10.1016/S0031-0182\(03\)00663-1](https://doi.org/10.1016/S0031-0182(03)00663-1).
- Underwood, C.J., and Rees, J., 2002, Selachian faunas from the lowermost Cretaceous Purbeck Group of Dorset, southern England: Special Papers in Palaeontology, v. 68, p. 83–101.
- Valenciennes, A., 1822, Sur le sous-genre Marteau, *Zygaena*: Mémoires du Muséum d’Histoire Naturelle, v. 9, p. 222–228, pls. 1, 2.
- von Bertalanffy, L., 1938, A quantitative theory of organic growth (inquiries on growth laws 2): Human Biology, v. 10, p. 181–213.
- Vullo, R., Guinot, G., and Barbe, G., 2016, The first articulated specimen of the Cretaceous mackerel shark *Haimirichia amonensis* gen. nov. (Haimirichidae fam. nov.) reveals a novel ecomorphological adaptation within the Lamniformes (Elasmobranchii). Journal of Systematic Palaeontology, v. 14, no. 12, p. 1003–1024, <https://doi.org/10.1080/14772019.2015.1137983>.
- Walliser, E.O., and Schöne, B.R., 2020, Paleogeography of the Late Cretaceous northwestern Tethys Ocean: Seasonal upwelling or steady thermocline? PLoS One, v. 15, no. 8, p. e0238040, <https://doi.org/10.1371/journal.pone.0238040>.
- Welton, B.J., and Farish, R.F., 1993, The Collector’s Guide to Fossil Sharks and Rays from the Cretaceous of Texas: Lewisville, Texas, Before Time, 204 p.
- Werner, C., 1989, Die Elasmobranchier-Fauna des Gebel Dist Member der Bahariya Formation (Obercenoman) der Oase Bahariya, Ägypten: Palaeo Ichthyologica, v. 5, p. 1–112.
- Whitley, G.P., 1939, Taxonomic notes on sharks and rays: Australian Zoologist, v. 9, p. 227–262.
- Wilkinson, I.P., 2011, Foraminiferal biozones and their relationship to the lithostratigraphy of the Chalk Group of southern England: Proceedings of the Geologists’ Association, v. 122, no. 5, p. 842–849, <https://doi.org/10.1016/j.pgeola.2011.10.002>.
- Witzmann, F., Haridy, Y., Hilger, A., Manke, I., and Asbach, P., 2021, Rarity of congenital malformation and deformity in the fossil record of vertebrates—A non-human perspective: International Journal of Paleopathology, v. 33, p. 30–42, <https://doi.org/10.1016/j.ijpp.2020.12.002>.
- Woodward, A.S., 1889, Catalogue of the Fossil Fishes in the British Museum, Part 1 Containing the Elasmobranchii: London, British Museum (Natural History), 474 p.
- Woodward, A.S., 1902, The fossil fishes of the English Chalk, part 1: Monographs of the Palaeontographical Society, London, v. 56, p. 1–56.
- Woodward, A.S., 1903, The fossil fishes of the English Chalk, part 2: Monographs of the Palaeontographical Society, London, v. 57, p. 57–96.
- Woodward, A.S., 1907, The fossil fishes of the English Chalk, part 3: Monographs of the Palaeontographical Society, London, v. 61, p. 97–128.
- Woodward, A.S., 1908, The fossil fishes of the English Chalk, part 4: Monographs of the Palaeontographical Society, London, v. 62, p. 129–152.
- Woodward, A.S., 1909, The fossil fishes of the English Chalk, part 5: Monographs of the Palaeontographical Society, London, v. 63, no. 308, p. 153–184.
- Woodward, A.S., 1911, The fossil fishes of the English Chalk, part 6: Monographs of the Palaeontographical Society, London, v. 64, p. 185–224.
- Woodward, A.S., 1912, The fossil fishes of the English Chalk, part 7: Monographs of the Palaeontographical Society, London, v. 65, no. 320, p. 225–264.

Accepted: 13 March 2022

Appendix 1. Corrections to tooth measurements of MPPSA IGVR 91032 (in mm). The numbers of teeth are those reported by Amalfitano et al. (2017a, fig. 6). CH = crown height; CT = crown thickness (labiolingual); CW = crown width; DCL = distal cutting-edge length; LCH = cusplet height; MCL = mesial cutting-edge length; PCH = central cusp height; PCW = central cusp width; TH = tooth height; TT = tooth thickness (labiolingual); TW = tooth width. Gray-shaded cells are those corrected.

Tooth	TH	TW	TT	CH	CW	CT	LCH	PCH	PCW	MCL	DCL
3	69	52	22	56	46	16	16	39	27	42	41
6	41	-	21	33	-	10	-	24	17	-	-
16	48	36	10	34	25	6	11	22	14	26	24

Appendix 2. Tooth measurements of BMB 007312 (in mm). The table includes measurements of some of the best-preserved teeth. CH = crown height; CT = crown thickness (labiolingual); CW = crown width; DCL = distal cutting-edge length; LCH = cusplet height; MCL = mesial cutting-edge length; PCH = central cusp height; PCW = central cusp width; TH = tooth height; TT = tooth thickness (labiolingual); TW = tooth width; * = tooth isolated from the matrix.

Tooth	TH	TW	TT	CH	CW	CT	LCH	PCH	PCW	MCL	DCL
a2	51	36	20	47	33	11	8	38	22	50	49
l2?*	-	-	-	-	-	12	-	29	19	-	-
a1	-	-	-	-	-	11	-	38	22	-	-
L1?	-	-	-	26	19+	6	4	18	14	-	25
L8?	19?	-	-	16	20?	-	4	13	10	-	16

Appendix 3. Placoid scale measurements of *Cretodus crassidens* (Dixon, 1850).

Sample	Scale location	Ridge spacing (μm)	Scale width (μm)
IGVR 91032	unknown	88-123-162	433
		99-113-92	711
		78-83-93-58-60-89	548
		82-138-105-137-86-76	694
		49-50-46-76-116-88-49-74-65-25	497
		115-115-81-59	600
		69-130	451
mean (n = 7)		87.32 \pm 30.65	562 \pm 103.31